NTNU – Trondheim
Norwegian University of
Science and Technology

Experimental investigations of the interaction between sea-ice and berm breakwaters

Daniel Miravalles Diez

Coastal and Marine Civil Engineering
Submission date: Januar 2013
Supervisor: Raed Khalil Lubbad, BAT
Co-supervisor: Alf Tørum, BAT

Norwegian University of Science and Technology
Department of Civil and Transport Engineering

NORWEGIAN UNIVERSITY OF SCIENCE AND TECHNOLOGY
DEPARTMENT OF CIVIL AND TRANSPORT ENGINEERING

Report Title: Experimental investigations of the interaction between sea-ice and berm breakwaters	Date: 15/01/2013 Number of pages (incl. appendices): 60			
	Master Thesis	X	Project Work	
Name: Daniel Miravalles Diez				
Professor in charge/supervisor: Raed Lubbad				
Other external professional contacts/supervisors: Alf Tørum				

ABSTRACT

The increasing interest on the Arctic areas has brought us new challenges that have not been met before in other locations due to the peculiarities of these latitudes. In this thesis the interaction between sea-ice and berm breakwaters has been studied.

This work introduces new variables to the study of this interaction that have not been reported before, including higher interaction velocities and 3D effects, by varying the ice concentrations and sizes of the ice floes. The other variables tested were the breaking length, thickness and roughness of the ice.

To reproduce this interaction, experimental investigations were carried out at NTNU and earlier setups were improved. The ice was modelled with paraffin and pushed against a scaled model of Sirevåg berm breakwater in a flume. The tests were modelled according to Froude scaling law, 1:70.

The ice and the breakwater behaviour were analysed and evaluated in relation to the parameters of the ice floes and new findings have been reported.

The speed did not have a strong influence on the forces exerted on the breakwater, but it increased the occurrences of ice stacking over the slope and the likeliness of local failures. These local failures invited to reconsider the suitability of no-reshaped berm breakwaters when facing sea-ice.

The accretion of ice rubble in front of the breakwater was reported as an effective barrier against the incoming ice.

Finally, when introducing the 3D effects with circular ice floes at concentrations around 8/10, the result was always an ice accumulation over the slope of the breakwater, forming ice rubble that protected the structure and did not cause any apparent damage.

As a recommendation for further work, improvements should be done to avoid the constraints caused by the flume walls.

Keywords:

1. Berm breakwaters
2. Sea-ice
3. Experimental investigation

(Signature) _____

NTNU
Fakultet for ingeniørvitenskap og teknologi
Institutt for bygg, anlegg og transport

MASTER DEGREE THESIS

Autumn 2012

for

Daniel Miravalles Diez

Experimental investigations of the interaction between sea-ice and berm breakwaters

Goals

The goal is to study the actions and the actions effects from sea-ice on berm breakwaters.

Gaps

Berm breakwaters could be considered as a good solution for the protection of harbours, artificial islands and shorelines in the Arctic areas because of the pile-up effect, which may reduce the incoming ice actions and also increase the overall stability of the breakwater.

A good understanding of the interaction between sea-ice and berm breakwaters will help to optimize the design of these structures in the Arctic. In order to improve our comprehension and knowledge, research must be conducted to estimate 1) the global ice actions, 2) the global response of the breakwater to ice actions and also to the combined actions from ice and waves, 3) the local ice actions and finally 4) the individual armour stones behaviour.

Research tasks

Mennessier (2012) carried out a model-scale 2D experiment to study the interaction between berm breakwaters and ice.

In this master thesis, the student will improve the experimental setup of Mennessier (2012) by including higher interaction velocities and to study the global failure of the berm breakwater under ice actions. Also, the student will include the 3D effects in his experiment by varying the ice concentrations and the sizes of the ice floes.

The student will discuss his experimental results and compare them with previously published results.

References

Mennessier, T. (2012): Berm Breakwaters as Protection of Harbours, Artificial Islands and Shorelines in Arctic Areas, Master Thesis, Norwegian University of Science and Technology, Department of Civil and Transport Engineering, June 2012.

General about content, work and presentation

The text for the master thesis is meant as a framework for the work of the candidate. Adjustments might be done as the work progresses. Tentative changes must be done in cooperation and agreement with the professor in charge at the Department.

In the evaluation, thoroughness in the work will be emphasized, as will be documentation of independence in assessments and conclusions. Furthermore the presentation (report) should be well organized and edited; providing clear, precise and orderly descriptions without being unnecessary voluminous.

The report shall include:

- Standard report front page (from DAIM, http://daim.idi.ntnu.no/)
- Title page with abstract and keywords.(template on: http://www.ntnu.no/bat/skjemabank)
- Preface
- Summary and acknowledgement. The summary shall include the objectives of the work, explain how the work has been conducted, present the main results achieved and give the main conclusions of the work.
- Table of content including list of figures, tables, enclosures and appendices.
- If useful and applicable a list explaining important terms and abbreviations should be included.
- The main text.
- Clear and complete references to material used, both in text and figures/tables. This also applies for personal and/or oral communication and information.
- Text of the Thesis (these pages) signed by professor in charge as Attachment 1.
- The report must have a complete page numbering.

Advice and guidelines for writing of the report is given in: "Writing Reports" by Øivind Arntsen. Additional information on report writing is found in "Råd og retningslinjer for rapportskriving ved prosjekt og masteroppgave ved Institutt for bygg, anlegg og transport" (In Norwegian). Both are posted on http://www.ntnu.no/bat/skjemabank.

Submission procedure

Procedures relating to the submission of the thesis are described in DAIM (http://daim.idi.ntnu.no/). Printing of the thesis is ordered through DAIM directly to Skipnes Printing delivering the printed paper to the department office 2-4 days later. The department will pay for 3 copies, of which the institute retains two copies. Additional copies must be paid for by the candidate / external partner.

On submission of the thesis the candidate shall submit a CD with the paper in digital form in pdf and Word version, the underlying material (such as data collection) in digital form (eg. Excel). Students must submit the submission form (from DAIM) where both the Ark-Bibl in SBI and Public Services (Building Safety) of SB II has signed the form. The submission form including the appropriate signatures must be signed by the department office before the form is delivered Faculty Office.

Documentation collected during the work, with support from the Department, shall be handed in to the Department together with the report.

According to the current laws and regulations at NTNU, the report is the property of NTNU. The report and associated results can only be used following approval from NTNU (and external cooperation partner if applicable). The Department has the right to make use of the results from the work as if conducted by a Department employee, as long as other arrangements are not agreed upon beforehand.

Tentative agreement on external supervision, work outside NTNU, economic support etc.
Separate description to be developed, if and when applicable. See http://www.ntnu.no/bat/skjemabank for agreement forms.

Health, environment and safety (HSE) http://www.ntnu.edu/hse
NTNU emphasizes the safety for the individual employee and student. The individual safety shall be in the forefront and no one shall take unnecessary chances in carrying out the work. In particular, if the student is to participate in field work, visits, field courses, excursions etc. during the Master Thesis work, he/she shall make himself/herself familiar with " Fieldwork HSE Guidelines". The document is found on the NTNU HMS-pages at http://www.ntnu.no/hms/retningslinjer/HMSR07E.pdf

The students do not have a full insurance coverage as a student at NTNU. If you as a student want the same insurance coverage as the employees at the university, you must take out individual travel and personal injury insurance.

Start and submission deadlines
The work on the Master Thesis starts on August 22nd, 2012

The thesis report as described above shall be submitted digitally in DAIM at the latest at 3pm January 15th, 2013

Professor in charge: Raed Lubbad

Other supervisors: Alf Tørum

Trondheim, August 22nd, 2012. (revised: . .)

_____

Professor in charge (sign)

ACKNOWLEDGEMENTS

This thesis is the end of a long road.

During the last few years I have had the opportunity to study in three different universities, in two different countries and meet a lot of professors, classmates and friends. In one or another way, all of them have contributed and helped me with my education.

Thanks to my family, who has always supported me.

Thanks to Raed Lubbad and Alf Tørum, my supervisors, for helping me and sharing their knowledge.

Thanks to Torgeir Jensen and Gustav Jakobsen, who helped me during the experimental work for this thesis.

Thanks to all my professors at NTNU, University of Alicante and University of Salamanca, who have taught me a lot during the last few years.

Thanks also to all the rest of the employees at NTNU, University of Alicante and University of Salamanca, who make the universities work and are always there to help the students.

Last but not least, thanks to all the people I did not mention but who were always there to answer the phone, solve any little problem or share a break.

TABLE OF CONTENTS

LIST OF FIGURES

LIST OF TABLES

1 INTRODUCTION

1.1 Background and motivation

The motivation to write this thesis comes from different sources. Taking the courses Marine Physical Environment and Port and Coastal Facilities during last year opened my eyes to a new event that I had never faced before: sea-ice. It was an amazing topic for someone coming from the south of Europe, where that is not a situation that you have to deal with in the coastal development of your home country. During the past summer, I enjoyed the opportunity to work in SAMCoT (Sustainable Arctic Marine and Coastal Technology), a Centre for Research-based Innovation. That experience strengthened my interest in ice-related topics, and brought me the opportunity to write this thesis.

Berm breakwaters could be considered as a good solution for the protection of harbours, artificial islands and shorelines in the Arctic areas because of the pile-up effect, which may reduce the incoming ice actions and also increase the overall stability of the breakwater. That gives the berm breakwaters an advantage when facing the ice in comparison with classical rubble mound structures, where the probability of the ice crossing over the top of the breakwater is higher.

A good understanding of the interaction between sea-ice and berm breakwaters will help optimizing the design of these structures in the Arctic. In order to improve our comprehension and knowledge, research has been conducted to estimate 1) the global ice actions, 2) the global response of the breakwater to ice action and also to the combined actions from ice and waves, 3) the local ice actions and finally 4) the individual armour stones behaviour.

This thesis was born with the objective of improving the experimental setup of Mennessier (2012) including higher interaction velocities and studying the global failure of the berm breakwater under ice actions. Another improvement is the inclusion of 3D effects in the experimental setup, by varying the ice concentrations and sizes of the ice floes.

Since the main focus was the relation between the force applied and the riding and piling up events, together with the potential failure of the breakwater, the model ice was substituted for paraffin. This election was first made by Mennessier (2012) and proved to represent the phenomena happening at full scale. The main advantages of the paraffin are that it doesn't require a cold laboratory and the simplification in the complicated task of scaling down the ice. The main limitation of the paraffin is the breaking mechanism of the ice in the breakwater, which was out the scope of this work.

While numerical analysis can show global failure of the structure, they can't show the movements of singular stones which are the most common incidents when the sea-ice arrives to the breakwater. This event can be analyzed with the scale model and documented with video, photographs and, in case of major damage, with a laser scanning.

1.2 Organisation of the report

The second chapter presents the theoretical background concerning the interaction between ice and both classical rubble mound and berm breakwaters. The differences between the two different design approaches can be observed, as well as the challenges that have to be faced in the Arctic areas when building breakwaters.

An explanation of the experimental setup used during the experiments can be found in the third chapter. It contains an explanation about physical modelling, a description of the instrumentation used, the data acquisition process, the model breakwater, the model ice, and a justification for the different decisions taken.

Chapter number four shows the discussion about the experimental work. The results obtained during the experiments are summarised, explained, analysed and compared with previous data. The different events concerning the model ice and the behaviour of the breakwater are presented, analysed and discussed.

The last chapter, number five, contains the corroborations and findings of the experiments. It also proposes some improvements for the experimental setup.

2 ICE INTERACTION WITH RUBBLE MOUND BREAKWATERS. THEORY AND PREVIOUS KNOWLEDGE.

2.1 Classical rubble mound breakwaters.

The initial scope of this thesis was the interaction between breakwaters and level ice, approaching to the breakwater as a single layer. However, during the experiments carried out with ice concentrations lower than 100% ice ridged were formed, which will be commented further in this document.

Most of the available literature regarding ice-breakwater interaction gives qualitative information. There are some points of view on the design of structures in Arctic areas and the required armour stone mass for these structures, like the ones proposed by Sackinger (1985), Chen and Leidersdorf (1988), or Timco et al. (1995).

However, there is a lack of quantitative analysis on this topic. Some investigations have been carried out concerning the required armour stone size, mainly as laboratory or model tests in ice tanks. Therefore, these tests may be subjected to scale effects (Tørum 2009).

Timco et al. (1995) and MacIntosh et al.(1995) reported different loading situations and failure modes after investigating the interaction between level ice and existing breakwaters. The different phenomena that may happen in the breakwater depends on the loading scenario, characterized by the ice flexural strength and thickness, the water depth, the slope inclination and the nature of the armour stones, according to the existing literature.

One of the aims of this work is to extend the knowledge about the loading scenario. To check if the speed of the ice and the concentration affects to the forces acting on the slope and the level of damage that it may cause.

When the sea-ice meets the structure, we can expect it to bend and break when it reaches its maximum flexural strength. The flexural strength is lower than the compression strength, which makes it the most probable failure model. Due to the use of paraffin as model ice, the failure models and ice properties, such as the flexural strength are out of the scope of this work. Different situations can follow this event. The ice may be pushed along the slope and ride-up, reaching or not the rear side (Figure 1). During the ride-up the pieces of broken ice can be form a pile of rubble on the slope (Figure 2), which maximum height depends on the ice thickness and the water depth.

Local failures are expected on the structure during the ice crush, ride-up and piling events, such as plucking, sliding and bulldozing, as discussed by Timco et al. (1995).

The height of the ice rubble plays an important role. The incoming ice sheet will be pushed between the breakwater and the rubble. That means that the more rubble there is over the breakwater, the more the ice sheet will be pressed against the armour. That can lead to push individual rocks along the slope during the ride up.

Then, there will be a horizontal load over the breakwater due to the incoming ice sheet and a vertical load due to the accumulated ice-rubble.

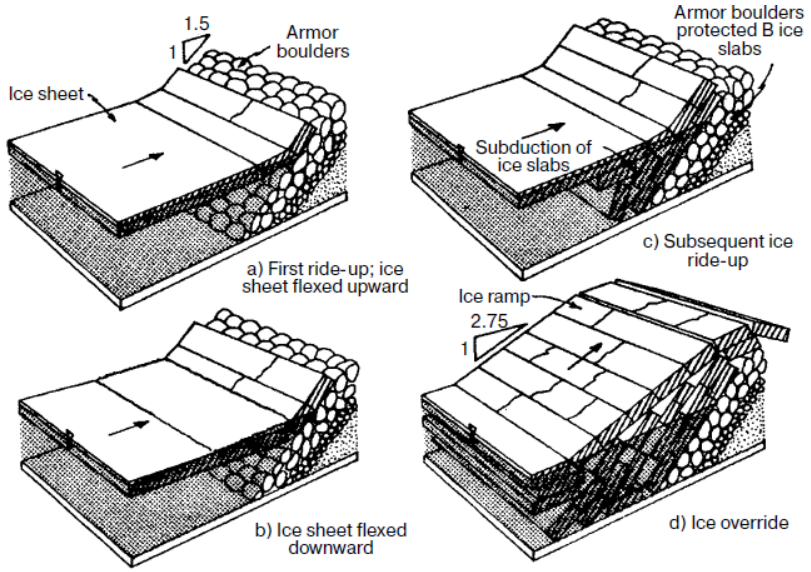

Figure 1 – Schematic of ice over-ride of an armour boulder protected side slope. Ettema et al. (1983).

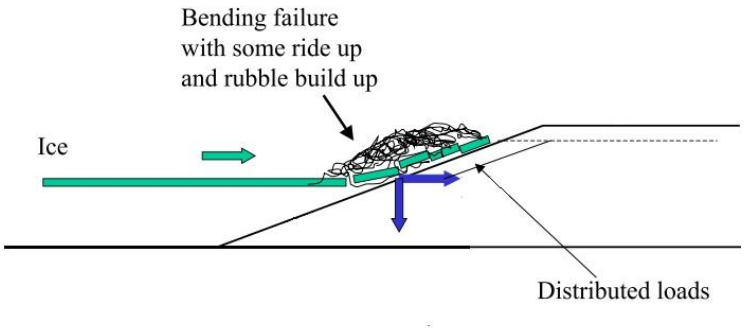

Figure 2 – Initial bending failure and ice ride up on rubble mound structure, Lengkeek et al (2003)

Another interesting fact happening in the contact between the ice and the breakwater was observed in the breakwaters at North Bay, Lake Nipissing (Ontario, Canada) by MacIntosh et al. (1995). "During the break-up, the ice melted away from the rocks before it moved off, so there was no potential for rafting or plucking". His belief is that the ice present in the interstices between the rocks may act as cement to help resist the external ice forces. This observation matches with the experiments carried out by Sodhi et al. one year later (1996). They observed that the underside of the ice sheet was shaved during its slide over of the riprap, filling in the interstitial spaces between the rocks, which smoothed the riprap surface.

The main damages observed in the breakwaters during the existing tests are displacements of individual stones. This doesn't represent a great danger for the structure itself, but it may be for the facilities that the breakwater protects when these rocks reach the top of the breakwater or override it.

With these considerations in mind, we can evaluate two different situations: with and without ice-rubble over the breakwater.

The situation without any ice-rubble accumulated in front of the slope leads to direct contact between the breakwater and the incoming ice. The irregularity of the breakwater's surface and the absence of any additional protection lead to some displacements of the rocks when the

first ice sheet hits the structure. The damage level observed due to this event observed during my experimental work is not severe. However, MacIntosh et al. (1995) observed that bulldozing can occur and cause extensive damage to a rubble mound structure, although they qualified this type of failure as "quite rare" (Figure 3).

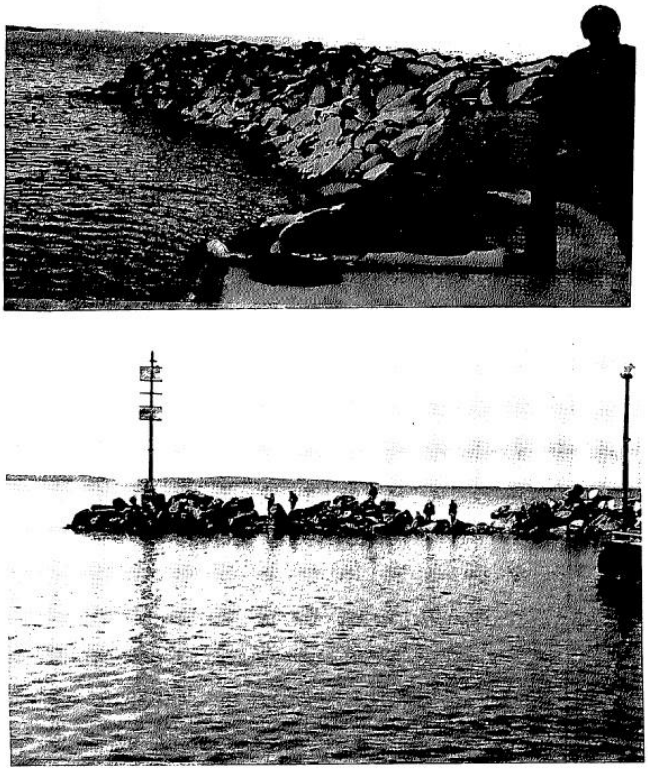

Figure 3 – Photographs showing the as-built and the ice-damaged breakwater at North Bay, Ontario, illustrating the "bulldozing" process. MacIntosh et al (1995).

This situation can occur during the early season, when ice starts growing and can reach a great thickness in short periods of time. However, it may also happen in the late season in case there is no previous ice-rubble accumulated over the slope.

On the other hand, the presence of an ice-rubble over the breakwater (which is more likely during the late season) has some advantages. Aside from the vertical load due to the accumulation of ice, it behaves as a protection for the rocks that otherwise have to face the incoming ice without any additional help. This avoids the local damage caused by the incoming ice sheets crushing against the slope and riding up. The damage is minimized if the ice rubble is consolidated and doesn`t slide along the slope.

The rubble field in front of the structure also increases the stability of the breakwater, although if the ice load is too big it could lead to global deep sliding of the structure (Mennessier 2012).

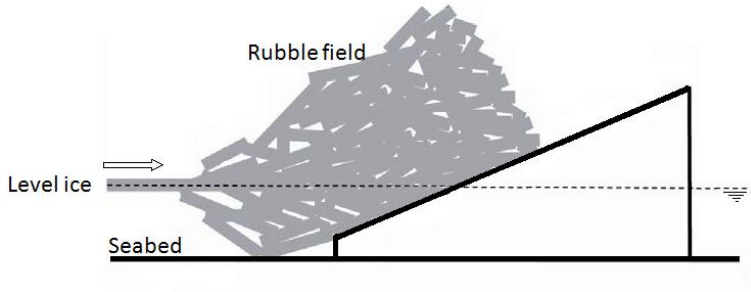

Figure 4 – Rubble field in front of the slope.

A good summary of the different failure scenarios are the three failure modes proposed by Lengkeek et al. (2003), associated with three different loading scenarios (Figure 5). These scenarios were proposed after some numerical modelling:

1) Local failure of the armour stone due to an ice sheet bending and riding up.
2) Global slip failure due to a thick ice sheet penetrating through the armour.
3) Global sliding due to a global distributed load from a consolidated rubble field in front of the structure.

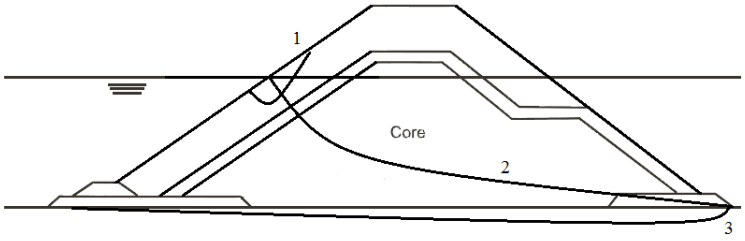

Figure 5 – Expected failure modes with different ice loads. Mennessier (2011).

Another aspect to consider is the size of the stones. During their investigations on small-scale tests, Sodhi et al. (1996) established a relation between the ice thickness-stones diameter ratio and the damage level, where the damage increases almost linearly with the h_i/D_{100} ratio. According to the results of Sodhi et al. (1996) there is no failure when h/D_{100} is smaller than approximately 0,5, while there is almost always failure if h/D_{100} is larger than 1,0. Sodhi et al. recommendations are less conservative than the ones provided by Ettema et al. (1986).

According to Daly et al. (2008), "selective placement is a more expensive method of construction than random placement, but the benefits are smaller stone size requirement and greater resistance to ice shoves". In the same study they evaluated the positive aspects of the presence of a toe in front of the structure, which improves the stability.

Regarding the cover layer, Lengkeek et al (2003) recommendation says that it should be at least one time the design ice thickness and the rock diameter should be about half the ice thickness. That implies that the cover layer should have at least two layers of rocks. This recommendation contradicts the previous results of Sodhi et al. (1996), which indicated that the rock size diameter should be 1 to 2 times the ice thickness.

Among Lengkeek et al. (2003) recommendations, they suggest the crest freeboard to be at least twice the ice thickness.

2.2 Berm breakwaters

When facing ice actions, berm breakwaters and classical rubble mound breakwaters face the same loading case scenarios. However, the structural behaviour is not the same.

The existence of a conventional rubble mound and a berm breakwater close to each other on the North Bay, Lake Nipissing (Ontario, Canada), gave MacIntosh et al. (1985) the opportunity to observe the differences in this behaviour. During one winter, there was significant damage done to the conventional breakwater when a moving ice sheet bulldozed a large section of the structure (Figure 3). The berm breakwater resisted better the ice forces, but it was not quantitatively analyzed. The annual ice thickness was around 0,7m and there was no information about the speed.

MacIntosh (1985) believes that "the flatter slopes at the waterline of a berm breakwater reduce the likelihood of rock movement by ice". While in a conventional rubble mound breakwater the ice bends and rides-up, the berm helps with the task of limiting the progression of the ice to the top and rear-side of the breakwater. When the ice reaches the berm it will most likely pile-up, preventing further damage caused by the incoming ice and the displaced rocks. "In addition, the berm itself can ground ice rubble for protection during the winter".

In fact, it is easier for the ice that has reached the berm to remain there than in a slope. This fact will provide the berm breakwater with a better stability compared with a conventional rubble mound breakwater. Sodhi et al (1996) also pointed out that the damage increases with the steepness of the slope.

The rubble mechanism was analysed by Gürtner (2009) during the SIB tests (further explanation later on), when he noted a structural dependence regarding the inclination of the shoulder. The ice was grounded faster for steeper shoulder inclination than for the shallower. However, when a limit inclination was reached the inclination of the shoulder became irrelevant. In this situation the rubble mechanism didn't contribute to increase the rubble height. It started developing towards the upstream side instead. After this condition was reached, no leeward over-riding of ice could be observed

These observations are valid for the ice actions during freezing and break up, but not during tidal actions due to Lake Nipssing's conditions.

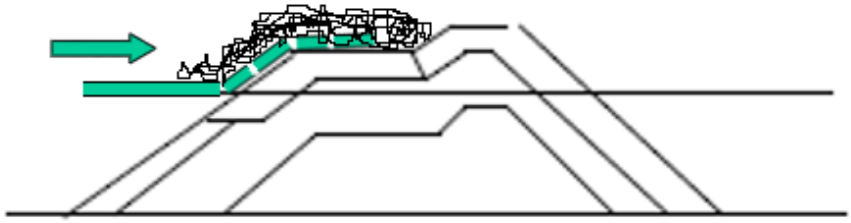

Figure 6 – Ice ride-up and pile-up on the berm (Mennessier 2011).

A similar design concept was proposed by Crosadale et al. (1988). They suggested building a bump in the slope of a beach. It would cause high bending stresses in the ice, which would break and pile up at the bump.

In the same line, Tørum (2004, in Tørum 2011) suggested that "a static stable berm breakwater, with such a bump built into it, would be suitable in Arctic areas where the structure is subjected to ice attack". Later, the tests of Daly et al. (2008) confirmed in a certain degree the advantages that a berm represents for ice barriers.

This concept was the seed to develop the "Shoulder Ice Barrier (SIB)", Gürtner (2009), Tørum et al. (2007). A 1:20 model of the structure (Froude's scaling) was built in the large ice tank of the HSVA (Hamburg Ship Model Basin) (Figure 7) with the purpose of protecting drilling platforms from ice in shallow waters. Although the SIB's shape is similar to a berm breakwater, this is a steel structure. That means that the surface of the structure is very different from the rocks present in a breakwater. Consequently it is not possible to evaluate the effects of roughness, selectively placement and local failures such as stone movements. However, they are expected to follow a similar pattern regarding the ice force.

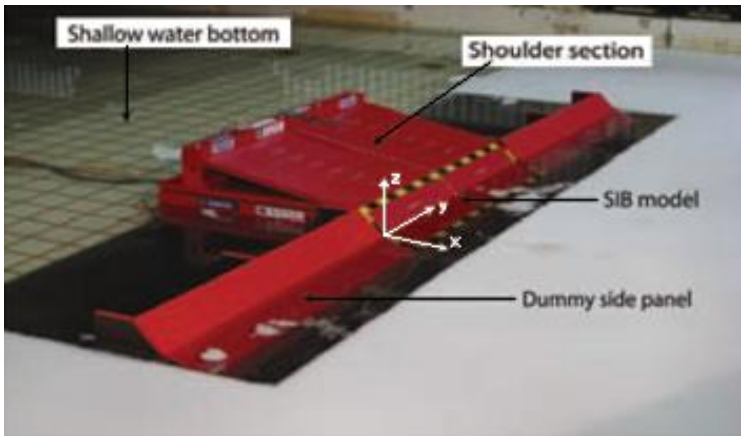

Figure 7 – SIB model in the HSVA ice model basin, Gürtner (2009)

The results of the force tests were reported by Gürtner (2009). He evaluated both horizontal and vertical forces and established a relationship between them.

The horizontal force was divided in three phases. The first one starts when the ice hits the structure and the force grows steadily. The second phase happens during the formation of the ice rubble over the structure. There are highly fluctuating forces with several peaks of short duration. Each of these peaks is preceded by a fast build up of the force levels. The peaks correspond with the failure events, when the force exceeds the flexural strength of the ice. After the peaks, the horizontal force decreases abruptly and a new build up event begins. Once the rubble is formed and it is grounded in front of the SIB, the third phase starts, characterized by a stationary and high force.

On the other hand, the vertical force increases steadily until it reaches a constant maximum force at the very end of the tests. During the first half of the run the vertical force is in the same order of magnitude than the horizontal force, while in the second half it is near twice the horizontal load.

Figure 8 represents the horizontal (a) and vertical (b) forces on the shoulder for one particular test run. It is possible to observe the different phases and connection between the forces commented previously.

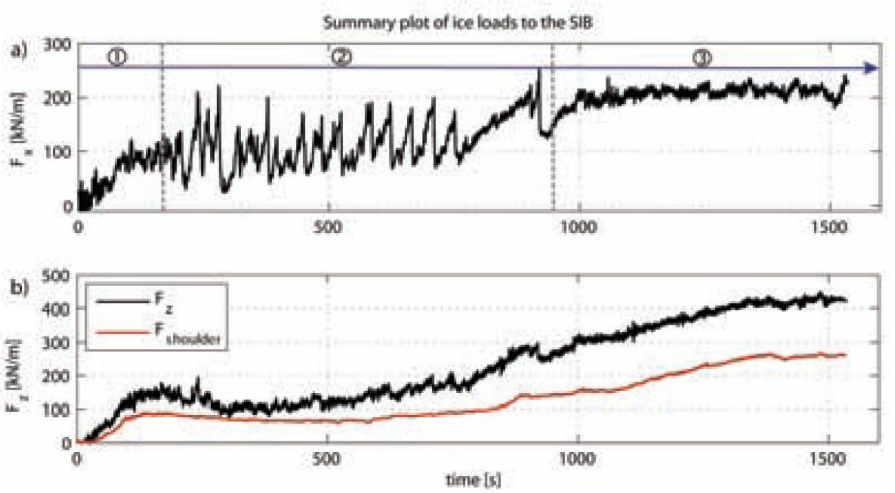

Figure 8 – Force summary plot of one particular test run with setup according to Figure 7, Gürtner (2009)

The highest load peaks were observed when the ice was pushing through the unconsolidated ice rubble at the structure and directly failing by crushing on the SIB surface. Forces were higher than observed in typical out-of-plane braking ice sheet due to the constraint of gravity and buoyancy on either side of the ice sheet.

Another aspect that should not be forgotten when designing a berm breakwater is that they are normally constructed with a berm that is allowed to reshape. This means that they can be designed either with a non reshaped static stable profile or with a reshaped (static or dynamic) stable profile. This needs to be considered when calculating the ice actions. Another concern in the design of a berm breakwater that is able to reshape is the excessive crushing and abrasion of individual stones as they move on the berm breakwater (Tørum 2011). However, the abrasion associated to the movements of stones pushed by the ice should not be something to worry in the reshaped profiles. On the contrary, it is considered as damage on non-reshaping berm breakwaters.

2.3 Ice action calculation for a rubble slope

There is not a detailed knowledge of the events following the contact between the sea-ice and berm breakwaters. This fact, together with the uncertainties related to the ice properties make difficult to predict the behaviour of the ice and propose some formulae to describe the events.

The ice impact on the slope was studied by Ettema et al (1983). They found that the forces exerted on side slopes by the ice sheets were lower than predicted for bucking of crushing failure. The reason was the non-simultaneous and irregular nature of the ice-sheet failure that occurs once the ice rubble has been accumulated along a side slope. They also came with an important contribution, since they established a relation between the maximum horizontal forces, per unit width of ice sheet, and the ice-sheet thickness.

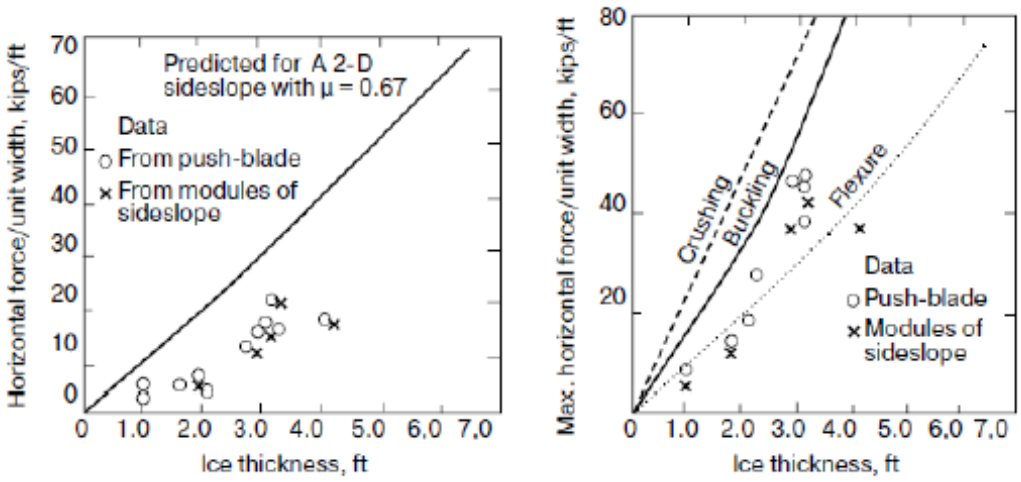

Figure 9 - Max. horizontal force per unit width of ice sheet during first ride-up event (to the left) and max. horizontal force per unit width of ice sheet during an entire test. After Ettema et al. (1983).

During their tests with a rip-rap model, Sodhi et al. (1996) observed that the maximum forces were associated with buckling. Although my experimental work has been carried out with paraffin instead of ice, I have observed that the maximum forces correspond to the events when two adjacent sheets bend and finally slide one over the other.

The standard ISO/FDIS 19906:2010(E) provides some formulae to calculate the ice load from level ice on a sloping structure. Since sloping structures are more likely to make the incoming level ice break in bending, the proposed model is based on elastic beam bending. These formulae are only valid for a sloping structure (they do not consider the berm) and do not consider the stone displacements either. The ice-structure interaction is simplified with the processes illustrated in Figure 10.

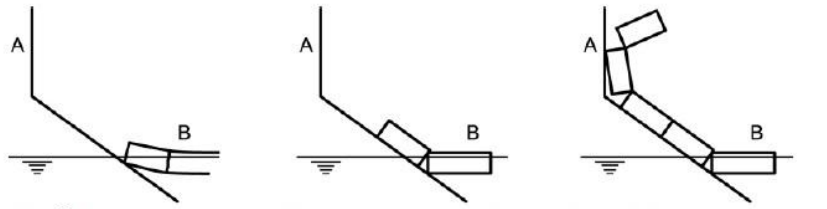

Figure 10 – Processes in the interaction between a sloping structure and ice sheet, ISO/FDIS 19906:2010(E).

Figure 11 sketches the ice action components evaluated in the formulae below.

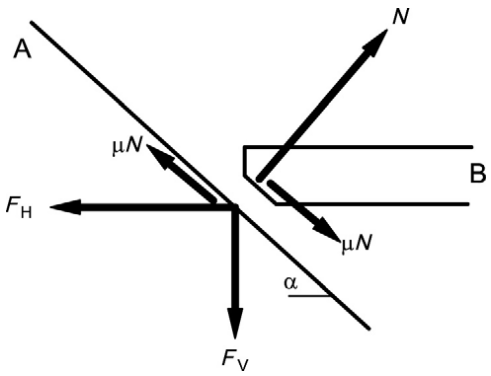

Figure 11 – Ice action components on a sloping structure for a two-dimensional condition, ISO/FDIS 19906:2010(E)

Key

A	sloping face of structure;
B	encroaching ice sheet;
N	normal component of reaction to ice action on structure;
μ	ice-structure friction coefficient;
α	slope of structure face from horizontal;
F_H	horizontal component of ice action;
F_V	vertical component of ice action.

The horizontal action component is determined as

$$F_H = \frac{H_B + H_P + H_R + H_L + H_T}{1 - \frac{H_B}{\sigma_f \, l_c \, h}} \tag{1}$$

Where H_B is the horizontal action due to ice breaking, H_P is the load component required to push the ice sheet through the ice rubble, H_R is the load to push the ice blocks up the slope through the ice rubble, H_L is the load required to lift the ice rubble on top of the advancing ice sheet before it breaks and H_T is the load to turn the ice block at the top of the slope. σ_f is the flexural strength of the ice sheet and h is the thickness of the ice sheet.

The relationship between the vertical and the horizontal components is

$$F_V = \frac{F_H}{\xi} \tag{2}$$

Where

$$\xi = \frac{\sin\alpha + \mu\cos\alpha}{\cos\alpha - \mu\sin\alpha} \tag{3}$$

The load component H_B is obtained from

$$H_B = 0.68\,\xi\,\sigma_f \left(\frac{\rho_w\, g\, h^5}{E}\right)^{0.25} \left(w + \frac{\pi^2\, L_c}{4}\right) \tag{4}$$

Where

$$L_c = \left(\frac{E h^3}{12\,\rho_w\, g\,(1-\nu^2)}\right)^{1/4} \tag{5}$$

Where E is the elastic modulus of the ice, ν is the Poisson ratio (typical value 0.3), ρ_w is the density of the water, w is the width of the structure and g is the acceleration of gravity.

The load component H_P is expressed as

$$H_P = w\, h_r^2\, \mu_i\, \rho_i\, g\,(1-e)\left(1-\frac{\tan\theta}{\tan\alpha}\right)^2 \frac{1}{2\tan\theta} \tag{6}$$

Where h_r is the rubble height, μ_i is the ice-to-ice friction coefficient, ρ_i is the density of the ice, e is the porosity of the ice rubble and θ is the angle the rubble makes with the horizontal.

The load component H_R is given by

$$H_R = wP\frac{1}{\cos\alpha - \mu\sin\alpha} \tag{7}$$

$$\begin{aligned} P = {} & 0.5\,\mu_i\,(\mu_i+\mu)\,\rho_i\,g\,(1-e)\,h_r^2\,\sin\alpha\left(\frac{1}{\tan\theta}-\frac{1}{\tan\alpha}\right)\left(1-\frac{\tan\theta}{\tan\alpha}\right) \\ & + 0.5\,(\mu_i+\mu)\,\rho_i\,g\,(1-e)\,h_r^2\,\frac{\cos\alpha}{\tan\alpha}\left(1-\frac{\tan\theta}{\tan\alpha}\right) \\ & + h_r\,\mathrm{h}\,\rho_i\,g\,\frac{\sin\alpha+\mu\cos\alpha}{\sin\alpha} \end{aligned} \tag{8}$$

The load component H_L is given by

$$\begin{aligned} H_L = {} & 0.5\,w\,h_r^2\,\rho_i\,g\,(1-e)\,\xi\,\left(\tfrac{1}{\tan\theta}-\tfrac{1}{\tan\alpha}\right)\left(1-\tfrac{\tan\theta}{\tan\alpha}\right)+ \\ & 0.5\,w\,h_r^2\,\rho_i\,g\,(1-e)\,\xi\,\tan\phi\left(1-\frac{\tan\theta}{\tan\alpha}\right)^2+\xi\,c\,w\,h_r\left(1-\frac{\tan\theta}{\tan\alpha}\right) \end{aligned} \tag{9}$$

Where c and ϕ are the cohesion and the friction angle of the ice rubble.

The last load component H_T needed in Equation (1) is given by

$$H_T = 1.5\,w\,h^2\,\rho_i\,g\,\frac{\cos\alpha}{\sin\alpha-\mu\cos\alpha} \tag{10}$$

When there is high horizontal force acting on the ice sheet, it influences the flexural failure of the ice sheet. This is considered by using the calculated value of the horizontal action to modify the flexural strength as follows

$$\sigma_f^{(1)} = \frac{F_H}{l_c\,h} + \sigma_f \tag{11}$$

Where l_c is the total length of the circumferential crack, estimated as

$$l_c = w + \frac{\pi^2}{4} L_c \tag{12}$$

To understand the physical behaviour under the formulae and the uncertainties related to the estimation of the variables it is useful to classify them:

The structural variables α and w are known values; the ice properties are h, ρ_i , μ_i (which is difficult to estimate) and σ_f (which depends on θ, h_r and c); the ice-structure interaction provides μ; the ice-rubble geometrical properties are θ, h_r , that are not so difficult to find by observing, and e; and the ice-rubble mechanical properties are c and ϕ, which are difficult to estimate with accuracy.

The predictions of this model depend considerably on the accumulated rubble on the slope. They are also very sensitive to the angle of repose chosen for the rubble pile. The force to drive the oncoming ice through this rubble pile and up the slope increases rapidly with the volume of the accumulated ice-rubble. This force is then transmitted to the structure and is a component of the total ice action.

The presence of snow is another fact that brings uncertainties to the calculation. It affects to the ice-ice friction and structure-ice friction coefficients, the porosity or the ice-rubble and the ice-rubble mechanical properties. In the absence of snow the horizontal action due to ice breaking is the main component.

When there are high speed interactions, ISO/FDIS 19906:2010(E) mention that the failure mode can change from bending to shear. The ice thickness has less of an influence for shear failure than for bending failure. Therefore shear failure is more prevalent at higher thicknesses. That is due to the inertial effects, which potentially increase the global ice action. The ice actions on sloping structures depend on the drift velocity. Speed effect is rather complex and its magnitude depends on the slope angle, sloping surface roughness and the ratio between ice thickness and waterline structure width. The effects of drift velocity on the breakwater and the force's dependence on this parameter observed during my experimental work are analysed later in this work.

While these formulae are useful to check the global stability of the structure, they do not provide any information about local loads to evaluate local damages such a stone movements.

3 EXPERIMENTAL SETUP

This thesis was born with the objective of improving the experimental setup of Mennessier (2012) by including higher interaction velocities and studying the global failure of the berm breakwater under ice actions. Another improvement is the inclusion of 3D effects by varying the ice concentrations and sizes of the ice floes.

In order to continue with the line of research of Mennessier (2012) several tests have been conducted with the experimental setup used in his experiments, improving the instrumentation necessary to introduce the new variables into the investigation of the interaction between sea-ice and berm breakwaters.

The tests have been carried out in a 60cm wide flume. The ice, substituted for paraffin, has been pushed towards a model cross section of the Sirevåg berm breakwater. The force required to push the ice has been recorded with two force transducers located in the pushing plate. The tests have been modelled according to Froude scaling law, **1:70**. Every test has been also documented with video and photographs. A laser scan has been installed to use it in case of global failure is detected.

3.1 Physical modelling and scaling

Physical modelling is a very useful tool in coastal engineering. Mathematical modelling offers important simplifications, but that may cause effects that must be evaluated by physical modelling. Thus we can examine phenomena which are beyond our analytical skills on this field.

The aim of physical modelling is to create a scaled model that behaves in the same way as it would at prototype scale. For this purpose the model has to preserve the properties of the prototype, so they are in similitude with each other.

3.1.1 Prototype and model similitude

There are three types of similarity required to be met when we build a physical model: geometric, kinematical and dynamical. Each of these relations is characterized by a scaling factor, which is defined as the ratio between a specific property of the prototype and the same property of the model.

Geometrical similarity refers to the shape. It exists when all the corresponding linear dimensions have the same scale ratio, defined as

$$\lambda = {L_p}/{L_m} \tag{13}$$

Where the sub index *p* refers to the prototype and the sub index *m* refers to the model.

Kinematic similarity refers to the motion. It is a similarity of velocities. It "is achieved when the ratio between the components of all the vectorial motions for the prototype and the model

must be the same for all particles at all times" (Hudson et al. 1979 in Hughes, 1993). Considering a common time scale λ_t, for the study domain, it is possible to define other kinematical scales like a velocity scale as $\lambda_U = \lambda/\lambda_t$ or an acceleration scale as $\lambda_a = \lambda/{\lambda_t}^2$, which are valid for all the motion field (Martin Vide, 2006).

However, this λ_t is a theoretical value difficult to model. To achieve realistic results it is mandatory to analyse the causes of the motion. That brings us to d*ynamic similarity*, which exists for geometrical and kinematical similar systems if there is a similarity in the force between the prototype and the model. The following force contributions are of importance: inertia forces (F_i), viscous forces (F_v), gravitational forces (F_g), pressure forces (F_p), elastic forces in the fluid (F_e), and surface forces (F_s).

Nevertheless, there is no fluid that fulfils all force ratios requirements. For that reason it is important to identify which forces govern the physical process that we are going to test and which ones are negligible. Once we know this, we can choose the proper hydraulic criterion for the model.

In coastal engineering, the dominant driving forces of most of the problems are the gravitational and viscous forces, while the elastic forces in the fluid and the surface tension are relatively small. Consequently, the necessary condition for hydrodynamic similitude can be fulfilled with the similitude of Froude (inertia/gravity forces) or Reynolds (inertia/viscous forces) number in combination with geometric similarity (Hughes, 1993).

3.1.2 Froude scaling

Froude Number is a dimensionless number that expresses ratio of inertia to gravity forces. It is defined as:

$$Fr = \frac{U}{\sqrt{g\,L}} \tag{14}$$

Then, the Froude model criterion should be applied when the inertial forces are principally balanced by the gravitational forces. In order to satisfy this criterion, the Froude Number must be the same in the model and in the prototype:

$$\left(\frac{U}{\sqrt{g\,L}}\right)_p = \left(\frac{U}{\sqrt{g\,L}}\right)_m \tag{15}$$

In terms of scale ratios, the Froude Number criterion is:

$$\frac{\lambda_U}{\sqrt{\lambda_g\,\lambda}} = 1 \quad \text{or} \quad \lambda_{Fr} = 1 \tag{16}$$

Due to the nature of the physical processes happening around the breakwater, the experimental work carried out by Mennessier (2012) followed Froude scaling law. The physical model, which I also used during my experimental work, was scaled with a geometrical scale ratio λ, of 70. The density of the model ice and the full scale density were considered to be the same. For practical purposes, the gravitational scale is unity, so following

the Froude criterion it is easy to derive other kinematical and dynamical scales, collected in Table 1.
From now on, all the results and parameters given are given as model-scaled values unless specified otherwise.

Table 1 - Froude scaling multiplication factors

Physical parameter	**Dimension**	**Similitude ratio**
Length	[L]	$\lambda = 70$
Time	[T]	$\sqrt{\lambda} = \sqrt{70}$
Force	[M L T^{-2}]	$\lambda^3 = 70^3$

3.1.3 Scaling effects

As complete similitude does not exist, scale effects may occur. That may happen when the neglected forces become important or do not scale in the same ratio than the dominant force. In my experiments, where Froude scaling is applied, viscosity, elasticity and surface tension forces are note scaled correctly. What we must wonder is if this forces that are not so important at full scale, become relevant after scaling the model.

The forces regarding Reynolds criteria, which is the other most used scaling, are viscous forces. They are not a problem in the primarily and secondary armour layers, where the velocities are relatively high due to the permeability of these layers, which leads to high Reynolds numbers.

Scaling effects can be reduced by building a model as large as possible, but that is not always possible due to the constraints on the laboratory facilities.

3.2 The testing rig

3.2.1 The flume

The flume where the tests have been conducted is situated in the laboratory of the NTNU Department of Hydraulic and Environmental Engineering. Its width is 60 centimetres and only near 5 meters of its total length were needed to carry out the tests. The longitudinal direction of the flume is considered as the x-axis while the y-axis corresponds to the horizontal direction perpendicular to the flume. The flume is shown in Figure 12.

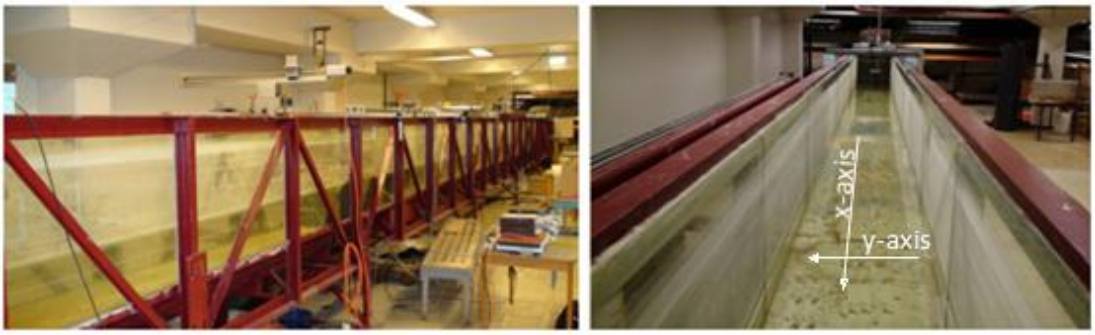

Figure 12-The flume

3.2.2 Towing carriage

A linear motion system was installed above the flume to move a plate that pushed the model ice against the breakwater in the x direction. The linear motion system used was Rollco QME30-2500, characterized by bearing shafts of 30mm diameter and a stroke length of 2500mm. It was calibrated prior to the tests and checked every tenth test.

To push the ice along the flume, a plate was hooked to the towing carriage with two jacks so it was able to push the ice along the x-axis.

The motor used to drive the towing carriage along the linear motion system was a step motor provided by SINTEF. With the configuration used for the experiments motor was able to push the model ice with a limit speed was 2.8 centimetres per second, corresponding to 0.23 meters per second at full scale. That was a great upgrade (28 times faster) compared to the setup used by Mennessier (2012), which allowed investigating the influence of the drift speed on the ice-breakwater interactions. However, it was not possible to drive the ice to desired maximum velocity of 0.5m/s (full scale). The force limitation came from the force transducers, so there was not necessary to push the motor characteristics to its limit in this regard.

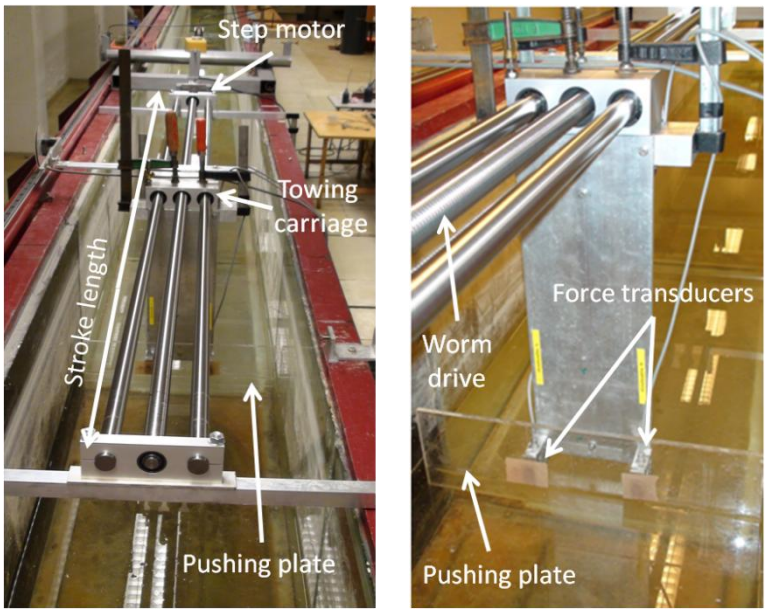

Figure 13 – Linear motion system (left) and pushing plate (right)

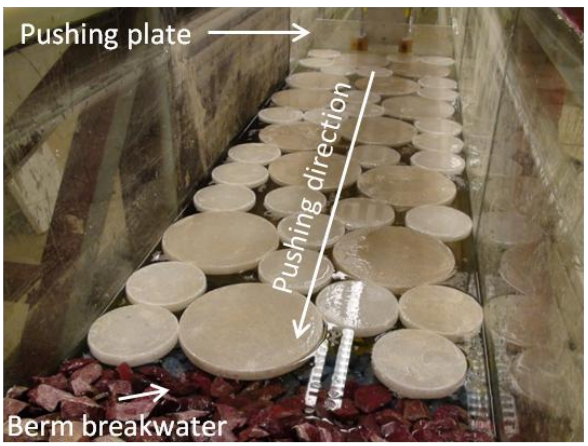

Figure 14 – Circular shaped model ice the flume ready to be pushed before test 57

3.2.3 Force transducers

In order to measure the force needed to push the ice, two force transducers were fixed symmetrically behind the plate that pushed the ice, registering the forces exerted in the x direction. The force transducers' type was S9M from HBM, which means S-shaped load cells for tensile and compressive forces. The serial numbers of the employed transducers were 30879157 and 30879164. The second one was replaced during some of the tests for a new one with serial number 300014720 due to some damage in the cable connecting it to the data logger. The nominal force of each of the force transducers was 500N and the accuracy class 0.02. The force transducers were calibrated according to the values provided by the manufacturer in the test certificate. They were also checked with two 1kg weights

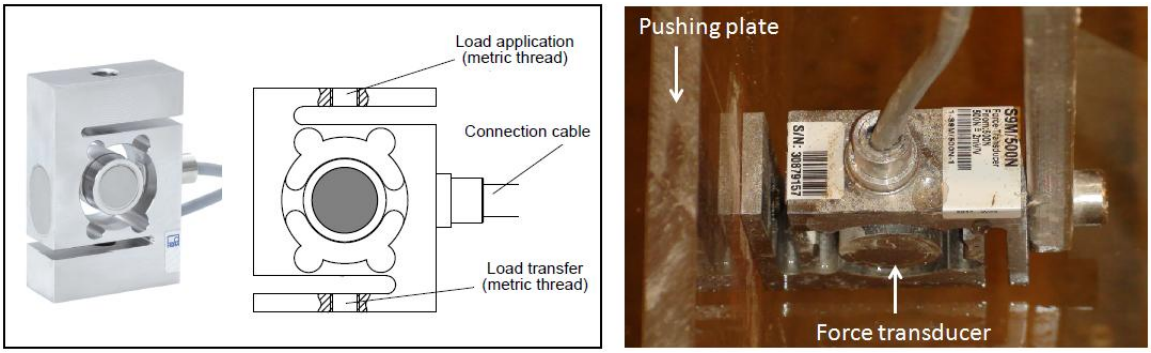

Figure 15-Force transducer principle (left) and detail of the installation (right)

3.2.4 Profiler

For the purpose of document any global failure or big deformations on the breakwater a profiler was installed by SINTEF. The data in the z-axis (height of the breakwater) was recorded with a laser SICK DME 2000, serial number 1010578. It was calibrated prior to use.

The laser was moved in the y direction thanks to a second step motor, while the movement along the x-axis was possible thanks to a bar that connected the linear motion system responsible to move the force transducers, that has been explained in section 3.2.2. The Figure 16shows the XY profiling system and the laser.

A drawback to the laser is that the water must be removed from the flume to scan the breakwater due to the light refraction. That implies a lot of time emptying and filling the flume between every test.

Figure 16-Profiling system and laser

3.2.5 Graphic documentation

Every test has been recorded with a high definition video camera in order to be able to visually analyse the model ice behaviour and the breakwater response in detail after each tests. Pictures of the breakwater have also been taken before, during and after every test in order to document any local failure and to show the behaviour of the ice over the breakwater.

3.2.6 Data acquisition and processing

The data acquisition process from the different sensors followed similar ways from the sensors until it was analysed and represented in the graphics.

The loads were measured with the force transducers described in section 3.2.3. Each transducer was connected via a single-channel amplifier plug-in module ML10B to an HBM MGCplus AB22A logger. The logger device was connected to a computer where the data were registered and displayed with the software Catman Easy (version 3.1) and exported in files ready to be analysed with MATLAB (version R2012b).

The position data followed two different paths. On the one hand, the x-distance data were registered with a linear encoder, which was connected to an analog-to-digital converter, after passing through a pulse-voltage converter. From this point they arrived to the HBM MGCplus AB22A logger and followed the same path than the load data. On the other hand, the y-distance data were registered with a step controller and digitally sent to the computer, where they were displayed with Catman Easy and analysed with MATLAB.

The height of the breakwater, z-distance, was registered with a laser, as described in 3.2.4. This device was directly connected to the computer, displayed with Catman Easy and analysed with MATLAB.

Finally, the time data were generated by the software Catman Easy for every test and it was analysed with MATLAB.

Figure 17 sketches the path followed by the data.

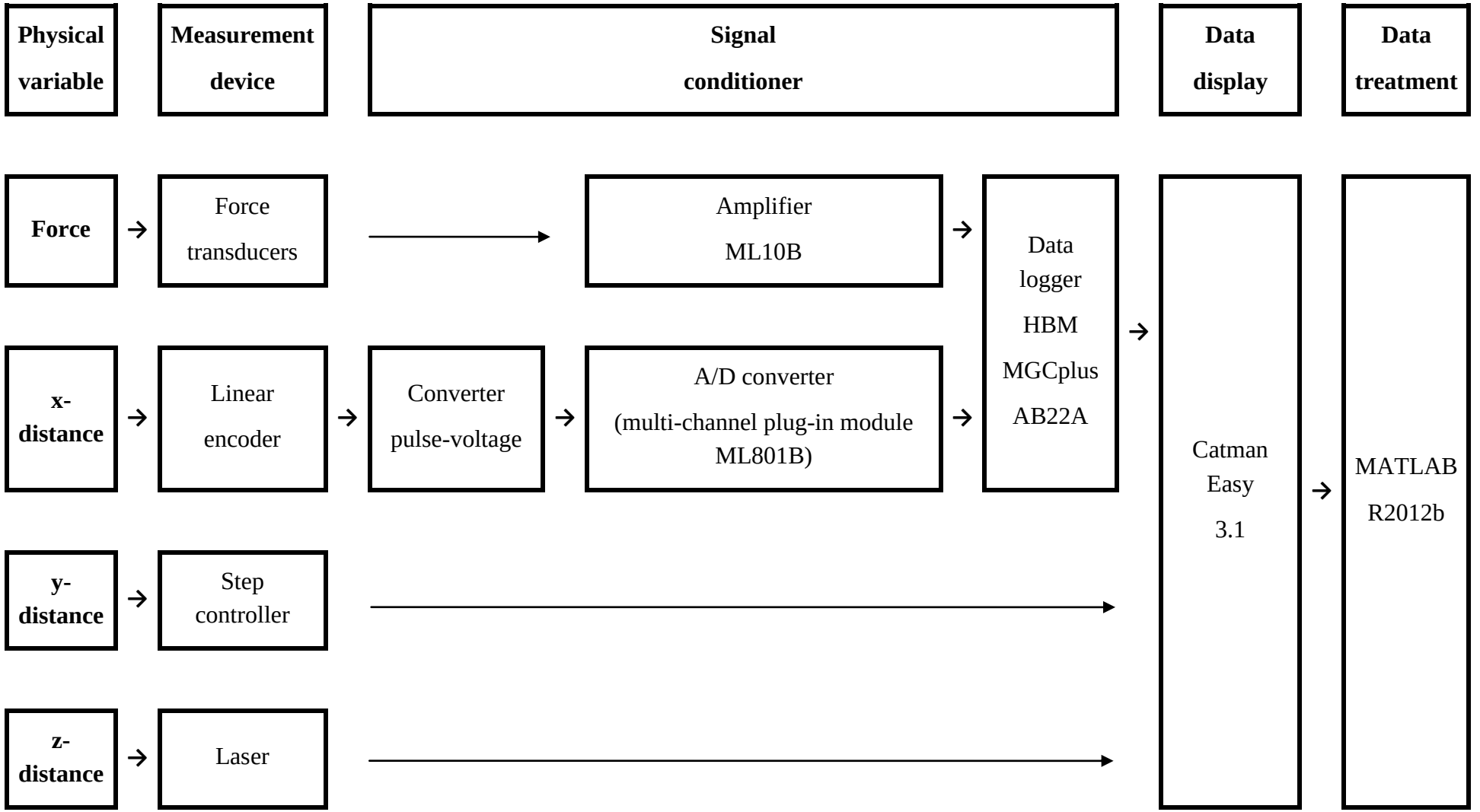

Figure 17 Data acquisition and treatment

3.3 The model berm breakwater

The berm breakwater design used to build the physical model utilized during the experimental work corresponds to Sirevåg berm breakwater. The location of the actual breakwater is 70km south of Stavanger, in Norway. The reason for the use of this design is to be able to give continuity to Mennessier (2012) work. That brought the opportunity to use an already built physical model (with some maintenance work), check the previous results and gain more in-depth knowledge of the mechanisms that occur between the sea-ice and the berm breakwater, having a similar previous study to compare the results.

The original reason of the use of Sirevåg berm breakwater was that it had been investigated in detail by Tørum et al (2003). The advantage of these studies is that its behaviour against the wave actions is well known.

Another benefit of the Sirevåg berm breakwater is the fact of being a non reshaping breakwater. That means that the profile of the breakwater is known before it is subjected to any ice action, which is an obvious benefit when it is necessary to carry out several tests on the same structure. When dealing with static stable reshaping berm breakwaters, they can be subjected to ice loads before or after they have reached their static shape.

The cross section of the built model is shown in Figure 18, while the characteristics of the stones are listed in Table 2. The model was installed in the flume, perpendicular to the x-axis previously defined. The flume floor was used as seabed, so the sand and rock bottom were not modelled.

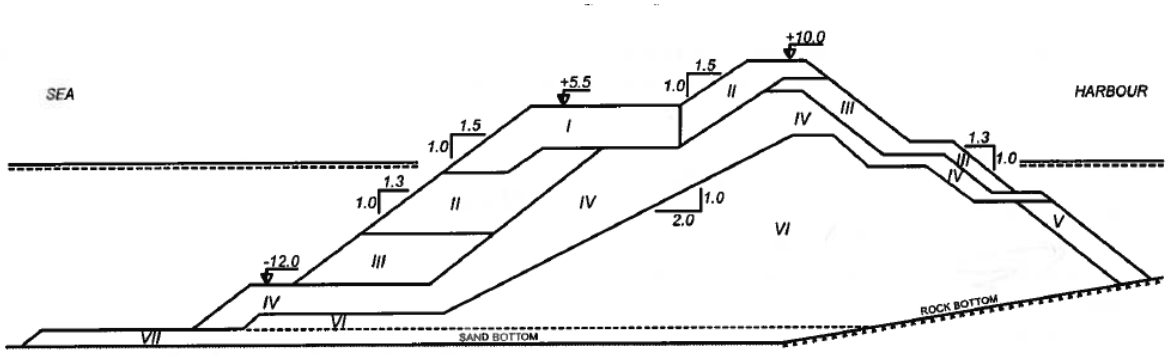

Figure 18-Cross section of the Sirevåg berm breakwater (Tørum et al. 2003)

Table 2 - Characteristics of the stones for the Sirevåg berm breakwater (Tørum et al. 2003)

	Stone class	**Prototype (tons)**	**Model (kg)**	**Gradation factor $f_g = D_{n85}/D_{n15}$**	**Mean volume reduction factor, k_{mean}**
$\rho_s = 2700kg/m^3$	I	20-30	0.058-0.087	1.11	0.41
	II	10-20	0.029-0.058	1.15	0.43
	III	4-10	0.012-0.029	1.20	0.42
	IV(filter)	$W_{50} = 1.6$	$W_{50} = 0.004$		
	V&VI (core)	$W_{50} = 1.2$	$W_{50} = 0.0036$		

3.4 The model ice

A singular fact of this experimental work is the use of broken pieces of paraffin instead of modelling the ice. This experimental setup was already used by Mennessier (2012), who proved that the different expected behaviour (rubble formation in front of the breakwater, riding up and piling up) can be observed with this material and is representative of some of the phenomena happening at full scale.

The use of paraffin provided the advantage of getting rid of some of the uncertainties that arise when modelling ice like the temperature play. It also helped because the same pieces of paraffin could be used for more than one test and made possible to carry out the tests without an ice tank.

To prepare the paraffin it was melted and shaped in rectangular and circular pieces simulating the already broken ice floes. It was not possible to simulate the breaking mechanism since the paraffin has different flexural and compression strength than the ice. That setup is valid because it is assumed that the breaking mechanism does not have a great influence in the piling and riding up events.

Different scenarios were recreated during the tests. For this purpose several parameters of the modelled ice floes were altered and combined during the experimental work. These were:

- the shape of the broken pieces,
- the length and diameter of the pieces (representing a breaking length),
- the thickness,
- the friction,
- the drift speed and
- the ice concentration.

In order to validate Mennessier`s (2012) work and compare the new tests run at higher speeds with the existing data, the different lengths and thicknesses of the rectangular pieces of paraffin tested were the same than the ones that he used during his tests. The used lengths were 7.5, 10.5, 13.5, 16.5, 19.5 and 22.5 centimetres, with thicknesses of 1.5 and 3cm. These thicknesses represent 1.05 and 2.10 meters at full scale, which are representative of medium and thick first-year ice respectively. While the breaking length of the paraffin may seem not too large (5.25 to 15.75m at full scale) compared with the ice floes found in nature, it was limited by the stroke length of the linear motion system and the width of the tank.

There were two different drift speeds used in the tests, 0.1 cm/s (the same one used by Mennessier (2012)) and 2.7cm/s.

The paraffin was tested with two different roughnesses. First, the tests were executed with the original roughness of the paraffin. Afterwards the tests were run with an added roughness, obtained by gluing sand to the surface of the model ice. The average grain size of the sand used was 150 micrometers. Due to the impossibility of remove the glued sand from the paraffin used in Mennessier's experiments, the tests with the rectangular ice floes were only run with the added friction. That was not a big inconvenience since Mennessier (2012) observed that the increased friction represented better the phenomena happening at full scale. "It led to less unrealistic pattern of the model ice and less unrealistic damage on the slope".

In the existing work the breaking length, the ice thickness and the roughness were the only parameters that could be varied. In order to introduce three dimensional effects to the test matrix, the concentration of the ice cover was varied during my tests. In the tests run with the rectangular ice floes, they had a width of 58cm, occupying the whole width of the flume. That resulted in 10/10 concentration. The variation of the concentration was possible thanks to the introduction of circular shaped ice floes with different diameters (13.5 and 22cm). The concentration was calculated as the ratio between surface of the ice cover during each test and the total water surface of the flume occupied during the corresponding test.

$$Surface\ of\ the\ ice\ cover = \sum_{i=1}^{n} n_i \frac{\pi\ {D_i}^2}{4} \tag{17}$$

Where *D* is the diameter of the ice floe and *n* is the number of ice floes with this diameter.

$$Water\ surface = W\ l \tag{18}$$

Where *W* and *l* are the width and the length of the water surface of the flume covered by ice.

$$Ice\ concentration = \frac{Surface\ of\ the\ ice\ cover}{Water\ surface} \tag{19}$$

While the initial idea was to vary the ice cover concentration by varying the number of circular shaped flows in the tank, when I tried to run the tests with low concentrations, the paraffin pieces were just pushed together until they reached a concentration over 8/10, occupying the whole length of the flume (except for the obvious gaps between the different pieces). During this gathering process there was no action on the breakwater, so the rests of the tests were directly run with initial concentrations around 8/10. The ice concentrations of the tests run with circular shaped floes are shown in Table 5.

Figure 19 – Aspect of the circular shaped model ice the flume before test 49

Table 4 sketches the groups of tests, which were named according to the floe characteristics and the drift speed of each test. The following pattern was used to easily identify the characteristics of a test just by watching the group to which the test belongs:

Table 3 - Categorisation of the tests

Position	Indicates	Values
First letter	Shape	R (rectangular) and C (circular)
First number	Thickness	1 (1.5cm) and 2 (3cm)
Second letter	Drift speed	L (low, 0.1cm/s) and H (high, 2.7cm/s)
Third to fifth letter	Breaking length or floe diameter	A (7.5cm), B (10.5cm), C (13.5cm), D (16.5cm), E (19.5cm) and F (22.5cm)
Last letter	Roughness	N (no friction) and F (d=150μm)

For example, tests number 23, 24 and 25 belongs to the group R2HA.F. That means that the ice floes were rectangular (R), the thickness was 3cm (2), the drift speed was 2.7cm/s (H), the breaking length was 7.5cm (A) and there was added friction of d=150μm (F).

If more than one letter is listed regarding the breaking length it denotes that ice floes from different sizes were used for that test. For example, in Test R1LABC.F breaking lengths of 7.4, 10.5 and 13.5cm were used together.

Table 4 - Groups of tests.

Shape		**Rectangular**			
Thickness (cm)		**1.5**		**3**	
Roughness (μm)		**150**		**150**	
Drift speed (cm/s)		**0.1**	**2.7**	**0.1**	**2.7**
Length (cm)	**7.5**	TestR1LABC.F (1)	TestsR1HABC.F (11,12,13)	TestR2LA.F (5)	TestsR2HA.F (23,24,25)
	10.5			TestR2LB.F (6)	TestsR2HB.F (26,27,28)
	13.5			TestR2LC.F (7)	TestsR2HC.F (29,30,31)
	16.5	TestR1LD.F (2)	TestsR1HD.F (14,15,16)	TestR2LD.F (8)	TestsR2HD.F (32,33,34)
	19.5	TestR1LE.F (3)	TestsR1HE.F (17,18,19)	TestR2LE.F (9)	TestsR2HE.F (35,36,37)
	22.5	TestR1LF.F (4)	TestsR1HF.F (20,21,22)	TestR2LF.F (10)	TestsR2HF.F (38,39,40)

Shape		**Circular**			
Thickness (cm)		**1.5**		**3**	
Roughness (μm)		**0**	**150**	**0**	**150**
Drift speed (cm/s)		**2.7**			
Diameter (cm)	13.5	TestsC1HC.N (41,42,43)	TestC1HC.F (60)	TestsC2HC.N (44,45)	TestsC2HC.F (55)
	22	TestsC1HF.N (46,47)	TestC1HF.F (61)	TestC2HF.N (48)	TestC2HF.F (56)
	13.5 and 22	TestsC1HCF.N (49,50,51)	TestsC1HCF.F (62,63,64)	TestsC2HCF.N (52,53,54)	TestsC2HCF.F (57,58,59)

Table 5 - Ice concentration on the tests

Shape		**Circular**			
Thickness (cm)		**1,5**		**3**	
Roughness (µm)		**0**	**150**	**0**	**150**
Drift speed (cm/s)		**2,7**			
Diameter (cm)	13,5	TestsC1HC.N (Test 41: 78.99% Tests 42-43: 84.63%)	TestC1HC.F (84.63%)	TestsC2HC.N (78.99%)	TestsC2HC.F (78.99%)
	22	TestsC1HF.N (75.21&)	TestC1HF.F (78.25%)	TestC2HF.N (78.25%)	TestC2HF.F (78.25%)
	13,5 and 22	TestsC1HCF.N (80.27%)	TestsC1HCF.F (80.27%)	TestsC2HCF.N (80.27%)	TestsC2HCF.F (80.27%)

3.5 Experimental procedure

The first step before running any test was the installation and calibration of the instrumentation described in the section 3.2.

Each group of tests has been repeated three times. There were two exceptions: the groups of tests already tested by Mennessier (2012), which were tested just once to check the results; and the tests with the circular shaped ice floes with just one floe diameter. The displayed setup provoked the formation of an ice ridge in front of the pushing plate. That, together with the wall constraints, resulted in extremely high forces on the plate that were not transmitted to the breakwater but to the flume walls.

The following pattern was repeated for every test.

Prior to each test, the breakwater was checked so it had the reference shape. Otherwise, the results could not be compared. The water level was also checked before every test.

After that, a bird's eye view picture of the breakwater was taken in order to compare it with one taken after the experiments and document any possible failure.

The next step was placing the pushing plate into its original position so there was enough room for the model ice. Once the model ice for the test was selected it was placed in the flume, between the pushing plate and the breakwater. During the tests with the circular shaped ice floes the ice concentration was calculated at this point.

When the model ice was in place, the force transducers and the linear encoder are zero-balanced. At this point the video camera, the data acquisition software and the software responsible to run the motor were ready to start. In the first place, the software to run the motor was activated. It was set up with a five seconds' delay, so there was some time to turn the data acquisition software and the video camera. This way the data, the graphs and the videos were synchronised.

During the experiment, the ice and breakwater behaviour were registered in a field notebook.

When the pushing plate arrived to the end of the stroke the motor stopped. That was the moment of taking some pictures of how the ice was accumulated in front or over the slope.

Afterwards, the ice was carefully removed and another bird-eye picture was taken in order to compare the condition of the breakwater with the original shape. In case of any global failure, the breakwater should be scanned and the new profile should be compared with the original one.

Finally, the pushing plate was brought to its initial position so a new test could be run.

4 DISCUSSION

As mentioned above, the aim of the experiments is to extend the knowledge we have about berm breakwaters on their potential use in Arctic areas. Two new parameters have been added to Mennessier (2012) work to delve deeper in the knowledge of the phenomena happening when a berm breakwater faces sea-ice: ice-drift velocity and ice concentration.

The analysis of this experimental work has been divided in three phases: the ice behaviour, the response of the breakwater and the analysis of the force signal. In the following pages, this will be analysed, focusing on the influence of the ice-drift velocity and the ice concentration.

4.1 Observed ice behaviour

The ice behaviour followed different patterns on the tests carried out with rectangular ice floes that in the ones carried out with circular ice floes.

The ice behaviour in the tests where rectangular shaped ice floes were tested followed the different behaviours observed by Mennessier (2012). However, the increase on the velocity changed the likeliness of some of them to happen, as described below. The phenomena observed during these tests were:

- Ride-up.
- Pile-up.
- Stacking.
  - Irregular ice rubble formation (described by Mennessier (2012) as "realistic stacking")
  - Cyclical ice rubble formation (described by Mennessier (2012) as "non-realistic stacking")

However, the tests carried out with the circular shaped floes followed a different pattern. First at all, the tests carried out with ice floes of the same diameter did not report any realistic result. The reason was that the constraints caused by the tank walls didn't allow the floes to move freely and reorganize. That brought to a completely unrealistic behaviour where ice rubble with a deep keel was formed in front of the pushing plate, as seen in Figure 20. The force transducers recorded extremely high peak loads due to this accumulation, but they were not transmitted to the breakwater at all. The cause of this behaviour is that the movement of the pushing plate was not transmitted to the ice placed in the proximities of the breakwater until the accumulated ice rubble formed in front of the pushing plate met that ice.

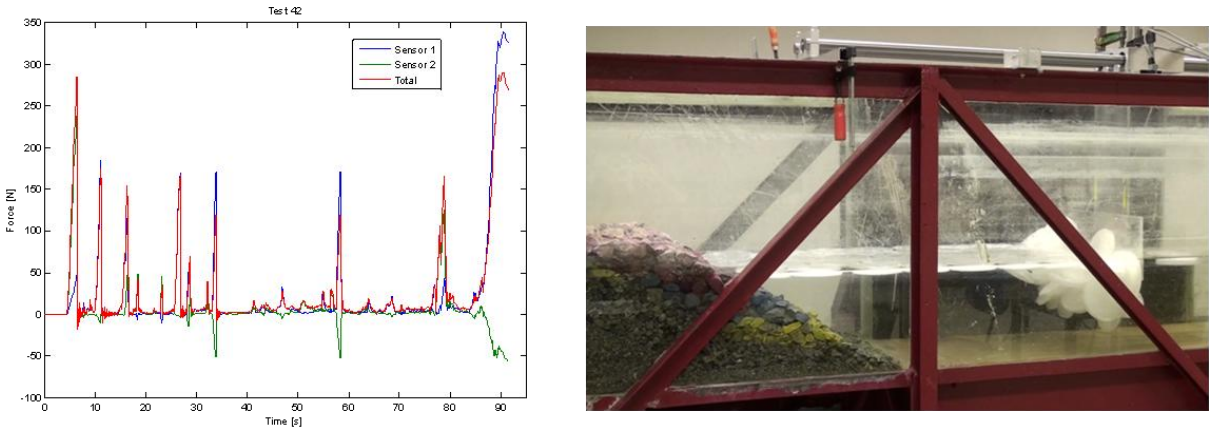

Figure 20 - Test 42: force-time graph and aspect of the test on second 54

Nevertheless, the mixture of ice floes with different diameters led to a more realistic behaviour. In all the tests carried out with this mixture the ice behaviour was very similar. Ice rubble was formed in front of the breakwater (Figure 21), acting as a barrier for the incoming ice. Therefore, none of the floes rode up to reach the berm. No damage was registered associated to this behaviour.

Figure 21 - Typical ice rubble formation in front of the breakwater during the tests with circular shaped ice. Test 57

The phenomena observed during rectangular shaped ice-floes tests are explained in the following paragraphs. Tables Table 6, Table 7, Table 8 and Table 9 compare the occurrence of the different phenomena for at different speeds. In these tables, in order to have the same number of events to compare, the occurrence of the events referring to the tests driven at 0.1cm/s refers to the results obtained by Mennessier (2012), where each cross represents a test where the analysed phenomenon happened. The occurrence of the events referring to the tests driven at 2.7cm/s refers to my own experimental work. The numbers on these tables refer to the number of times that each event happened during each group of tests.

4.1.1 Ride up

When a berm breakwater is built in environments where sea-ice is present, the ride up is the principal phenomenon to that should be controlled. At least to avoid that the ice rides up to the rear side of the slope, damaging the structures or objects that it should protect.

As seen in Table 6, the likeliness of this event increases with the thickness of the ice floes. That is due to the likeliness of the thin ice floes to slip over the following floe. When the thickness is bigger, the pushing surface is more stable, allowing the ice cover to act like a carpet, riding over the slope.

A very interesting fact is that the likeliness of the ride up happening depends also on the size of the ice floes and on the drift speed. The shorter is the breaking length of the ice floe the greater is the possibility of the ice to ride up the slope.

The drift speed has different consequences depending on the thickness of the ice floes. It does not affect to the likeliness of the ride up for the thin ice. A total of two ride up events were observed in the tests run at 0.1cm/s while three were observed during the ones run at 2.7cm/s. However, it seems to affect to the likeliness of the ride up if the thickness increases by decreasing it. An exception is noted when the ice floes have a small breaking length, which compensates the effect of the high speed. When the drift velocity is lower it seems the ice cover it is been pushed more carefully against the breakwater, so the breaking events are not so likely to happen, allowing the ice cover to ride over the slope.

A perfect example of a ride up event is test 23, shown in Figure 22 where the ice cover rode up the slope and reached the rear side. In this figure, the time force series perfectly captures the course of the events. After the ice hits the breakwater, the force grows steadily from second 4 to 21. After that, the formation of the ice rubble is reflected in high and fluctuating forces with several peaks of short duration. These peaks correspond to accumulation of a new ice floe to the rubble. This behaviour matches with the one observed by Gürtner (2009) during his experimental work with the SIB model in the HSVA, as described in 2.2.

There was also observed some pile up during this test, but it was too late to act as a barrier for the incoming ice as pretended.

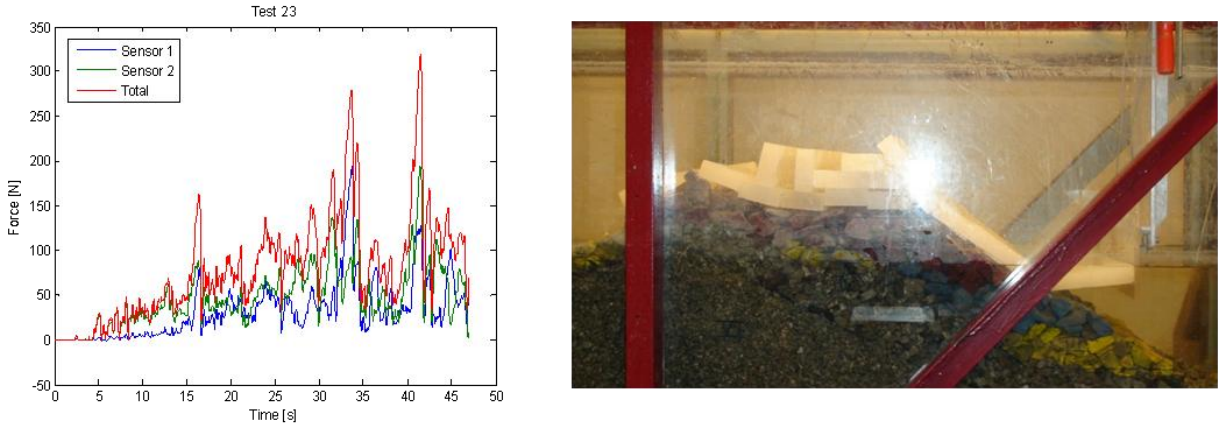

Figure 22-Test23: Typical ride up phenomenon

Table 6 - Occurrences of ride up

Shape		**Rectangular**			
Thickness (cm)		**1.5**		**3**	
Roughness (µm)		**150**		**150**	
Drift speed (cm/s)		**0.1**	**2.7**	**0.1**	**2.7**
Length (cm)	**7.5**	2	3	2	3
	10.5			1	2
	13.5			3	0
	16.5	0	0	1	1
	19.5	0	0	2	1
	22.5	0	0	1	0

4.1.2 Pile up

According to the literature review, the pile up events on the berm of the breakwater is the behaviour, caused by the berm that we look for when designing a berm breakwater in Arctic areas.

However, as shown in Table 7, the likeliness of this event is not very high. Nevertheless, when it happens, it has been observed to act as an effective barrier for the incoming ice. It is to note that in some situations, like the observed in test 23 (see Figure 22), the pile up acts as a barrier for the incoming ice, but cannot prevent the ice reaching the rear side of the breakwater because it may happen before the ice piles up on the berm. This particular behaviour, where the ice reaches the rear side of the slope, was observed only once during my tests run at 2.7cm/s and was not observed at all either during the tests run at 0.1cm/s by both Mennessier and me, so it is not very likely the ice to reach the rear side of the structure.

The effect of the speed on this behaviour is again different depending on the thickness of the incoming ice. On the one hand, it does not affect at all when dealing with thin ice, since the occurrence of the pile up events was exactly the same at both high and low speed tests. On the other hand, the effect of high speeds on thick ice floes depends again on the breaking length of the flow. At higher speeds the likeliness of the event happening is greater when the breaking length is shorter, but it decreases when we increase the breaking length.

Table 7 - Occurrences of pile up

Shape		**Rectangular**			
Thickness (cm)		**1.5**		**3**	
Roughness (µm)		**150**		**150**	
Drift speed (cm/s)		**0.1**	**2.7**	**0.1**	**2.7**
Length (cm)	**7.5**	1	1	1	2
	10.5			1	2
	13.5			1	0
	16.5	0	0	0	0
	19.5	0	0	1	0
	22.5	0	0	0	0

Test 28 is a perfect ambassador of the pile-up phenomenon. The aspect of the ice over the berm after the test can be observed in Figure 23, when the pile-up happened from second 23.

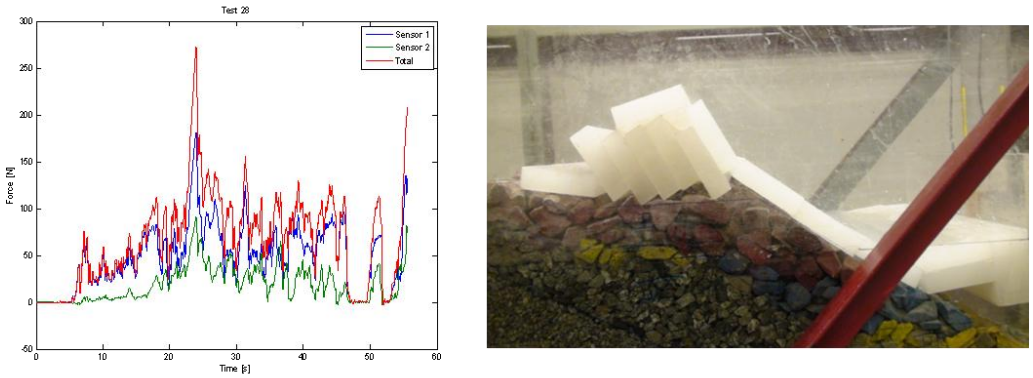

Figure 23-Test 28, representing pile-up over the berm of the breakwater.

4.1.3 Irregular ice rubble formation (described by Mennessier (2012) as realistic stacking)

This is the event that is most likely to happen. It occurs when a breaking event on the ice cover makes the ice start accumulating in front of the breakwater without a regular pattern.

This event is sometimes associated to ride up events. That happens when a single layer of ice is accumulated over the breakwater and it works as a softer ramp for the incoming ice to ride up. However, this accumulation can also provoke the opposite effect, which happens most of the times, when the ice rubble accumulated over the slope acts as very effective barrier to reduce the actions of the incoming ice over the breakwater (Figure 24). Table 8 shows the occurrences of this realistic stacking.

Table 8 - Occurrences of realistic stacking

Shape		**Rectangular**			
Thickness (cm)		**1.5**		**3**	
Roughness (µm)		**150**		**150**	
Drift speed (cm/s)		**0.1**	**2.7**	**0.1**	**2.7**
Length (cm)	**7.5**	2	3	1	2
	10.5			0	2
	13.5			2	2
	16.5	3	3	2	3
	19.5	2	3	3	3
	22.5	3	2	3	3

The paper of the speed on this behaviour seems to be more relevant when the ice thickness increases. In the tests run with 1.5cm thickness floes, there was not much difference between the tests run at different speeds. In those tests, independently of the size of the floes, the rubble formation occurred in a similar percentage of the tests: 10 out of 12 times during the tests run at 0.1cm/s, and 11 out of 12 times for the tests run at 2.7cm/s. However, during the tests carried out with 3cm thickness ice floes, there was a more noticeable increase in the occurrences when the velocity was higher, as can be observed in Table 8. While this kind of

staking was already prone to happen for the thick ice and the large floe lengths, the increase of the speed enlarged the occurrences for every floe length.

Figure 24-Accretion on the slope with (left) and without (right) previous ride up. Tests 24 (left) and 27 (right).

4.1.4 Cyclical ice rubble formation (described by Mennessier (2012) as "non-realistic stacking")

This is an uncertain behaviour with a very low recurrence, as compiled in Table 9. It is characterized by the accumulation of ice sheets in front of the slope, parallel to it. It happens when the contact between two floes plunges, forming a *V* flooded by water. The incoming floe slides over the previous one, leading to a situation like the one shown in Figure 25. A very characteristic time-force series is associated to this behaviour, where the force grows steadily until two contiguous ice floes slide over each other, causing a sudden release on the force which will grow again until the next slide. In real ice, the maximum force of the cyclic peaks of these graphs would correspond to the flexural strength.

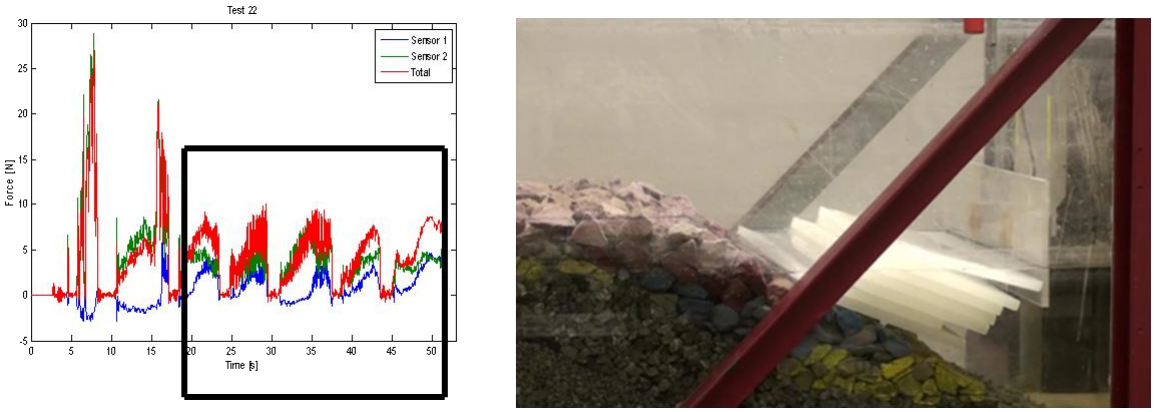

Figure 25-Test 22: non realistic accretion at the front of the breakwater

This behaviour seems to be influenced by random facts and the constraints of the tank walls, rather than by the drift speed or the thickness of the ice. Nonetheless it was not observed for the shortest breaking lengths. That can be due to the breaking pattern.

No damage was registered due to this behaviour, which acted as a very effective barrier for the incoming ice.

Table 9 - Occurrences of non realistic stacking

Shape	**Rectangular**	
Thickness (cm)	**1.5**	**3**
Roughness (µm)	**150**	**150**

Drift speed (cm/s)		0.1	2.7	0.1	2.7
Length (cm)	7.5	0	0	0	0
	10.5			0	0
	13.5			2	2
	16.5	0	0	0	0
	19.5	1	0	0	0
	22.5	2	1	0	0

4.2 Observed response from the breakwater

Many local failures have happened during the tests, but no global failure has been registered, being the maximum total force transmitted to the breakwater during the tests 362.5N during test 57. Higher peak loads were recorded during tests 43, 44, 55 and 56, but they were not transmitted to the breakwater since the cause was the ice rubble formation in front of the pushing plate, as explained in 4.1.

Mennessier (2012) categorized the failures as

- Armour stones rolled upward.
- Damage to the crest.
- Damage to the toe.

During my tests, many armour stones have been rolled upward, as shown in Table 10. The effect of the drift velocity is clear, provoking more local failures. However, it is to note that these failures have mainly happened due to the push of the first ice floe arriving to the berm breakwater. Once an ice layer was formed over the breakwater due to any of the described behaviours, it acted as a very effective protection for local damages.

While Mennessier observed some damage to the crest during his experimental work, this part of the breakwater was not damaged at all during my tests, which leads to think that the events caused by ice coming at high speed are less harmful for the crest.

Finally, the occurrence of the toe damage has been really low, as shown in Table 11. It has been caused by floes sliding down the slope due to a release on the force. This kind of damage should be even lower if we had operated with real ice attending to MacIntosh et al. (1995) observations, described in 2.1. His belief is that the ice present in the interstices between the rocks may act as cement to help resist the external ice forces.

In tables Table 10 **¡Error! No se encuentra el origen de la referencia.**and Table 11, which refer to my experimental work, letter T next to the number of the tests denotes that the stone has just tilted or turned but it has not suffered any displacement. Letter D denotes a displacement of one of more stones. If some stones have been displaced and others have just tilted the event is marked as D, as it is the greater damage.

Sirevåg berm breakwater has the peculiarity of being a non-reshaping berm breakwater. Therefore, any displaced stone is considered as a failure. Even the local failures are not very harmful, its high recurrence should make us reconsider the use of a non reshaping berm breakwater as a protection against the sea-ice.

Table 10 – Occurrence of local failure due to armour stones rolling upward

Shape		**Rectangular**			
Thickness (cm)		**1.5**		**3**	
Roughness (µm)		**150**		**150**	
Drift speed (cm/s)		**0.1**	**2.7**	**0.1**	**2.7**
Length (cm)	**7.5**	1T	11D ,13D	5D	23D, 24D, 25D
	10.5			6D	26T, 28D
	13.5				29T, 30D, 31T
	16.5		14T, 15D, 16D	8D	
	19.5		17D, 18D	9D	35D, 36D
	22.5	4D	20D		

Table 11 – Occurrence of local failure due to armour stones rolling down

Shape		**Rectangular**			
Thickness (cm)		**1.5**		**3**	
Roughness (µm)		**150**		**150**	
Drift speed (cm/s)		**0.1**	**2.7**	**0.1**	**2.7**
Length (cm)	**7.5**				
	10.5				
	13.5				30T
	16.5				34D
	19.5	3D	18T, 19D		36T
	22.5				40T

4.3 Analysis of the force signal

A key issue of this experimental work was to analyse the influence of the ice drift speed on the force tests. While it has a significant influence on the local damages, it does not seem to have a strong influence on the force registered by the force transducers compared with the detected at lower speeds. That may be due to the different likeliness of the breaking patterns to happen. Whereas for the smaller breaking lengths the velocity gives the impression to decrease the force (especially when the ice is thicker), this effect disappears when the breaking length increases, as can be observed in Figure 26.

In order to compare the forces detected in the tests run at low speed (0.1cm/s) by Mennessier (2012) and my experimental work, run at high speed (2.7cm/s), a statistical analysis has been done and shown in Table 12 and Figure 26. The maximal force data of each test was collected with MATLAB when the time-force graphs were elaborated. The arithmetic mean and the standard deviation of those maximal force data have been calculated for each group of tests.

The arithmetic mean gives the average of the analyzed values,

$$\bar{x} = \frac{1}{n}\sum_{i=1}^{n} x_i \qquad \text{[Arithmetic mean]} \qquad (20)$$

The standard deviation shows the dispersion from the average. In other words, how much variation exists from the mean value. It is to note that higher standard deviations were found for the tests run at high speed (2.7cm/s) with the thicker ice (3cm).

$$\sigma = \sqrt{\frac{1}{n}\sum_{i=1}^{n}(x_i - \bar{x})^2} \qquad \text{[Standard deviation]} \tag{21}$$

Table 12 – Mean maximal force in Newton for each series. Standard deviation is indicated in brackets

Shape		**Rectangular**			
Thickness (cm)		**1.5**		**3**	
Roughness (µm)		**150**		**150**	
Drift speed (cm/s)		**0.1**	**2.7**	**0.1**	**2.7**
Length (cm)	**7.5**	57 (21)	41 (16)	191 (20)	237 (59)
	10.5			162 (33)	218 (92)
	13.5			135 (13)	126 (36)
	16.5	28 (2)	22 (8)	101 (39)	113 (5)
	19.5	58 (32)	18 (7)	128 (13)	119 (47)
	22.5	33 (2)	19 (6)	79 (16)	86 (5)

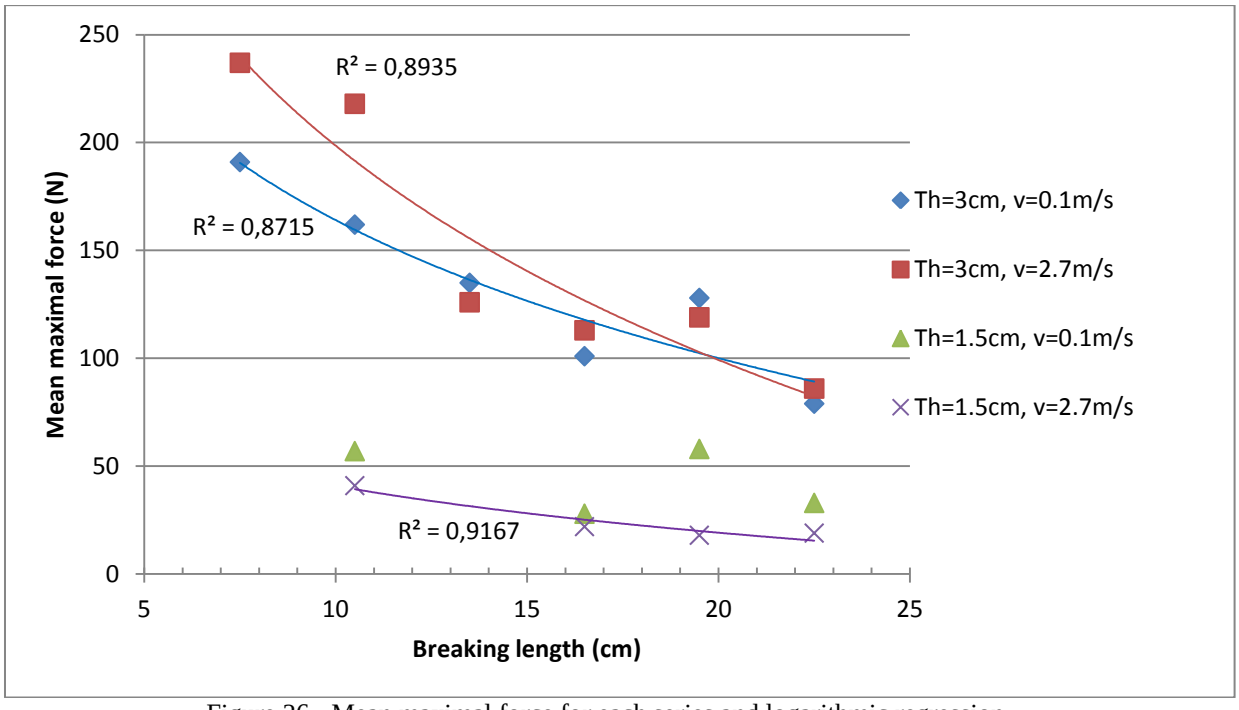

Figure 26 - Mean maximal force for each series and logarithmic regression

The graph above shows the relation between the breaking force and the breaking length. The logarithmic regression is the one that fits better with the data attending to Pearson product moment correlation coefficient, R^2.

$$R^2 = \frac{\sum(x - \bar{x})(y - \bar{y})}{\sqrt{\sum(x - \bar{x})^2 \sum(y - \bar{y})^2}} \tag{22}$$

The values from Table 12 can be compared with the ones obtained by applying the formulae proposed by ISO/FDIS 19906:2010(E), that have been explained in chapter 2.3. As example, parameters from tests 6 and 27, which where run with the same ice sheets but at different speeds, have been compiled and the horizontal force has been calculated. The use of these tests facilitates the calculations, since the ice rides up parallel to the slope of the breakwater. Therefore, the slope of the structure, α, and the angle the rubble makes with the horizontal, θ, are equal. That allows simplifying formula (1) for the horizontal action component since H_P (equation 6) and H_L (equation 9) are null, getting also rid of the estimation of the porosity, cohesion and friction angle of the ice rubble. As we have not considered the breaking mechanism and the model ice is already fractured before the tests start, $H_B = 0$.

With these considerations, the necessary equations to calculate the horizontal force are

$$H_R = w * h_r \, \mathrm{h} \, \rho_i \, g \frac{\sin\alpha + \mu\cos\alpha}{\sin\alpha} * \frac{1}{\cos\alpha - \mu\sin\alpha} \tag{23}$$

$$H_T = 1.5 \, w \, h^2 \, \rho_i \, g \frac{\cos\alpha}{\sin\alpha - \mu\cos\alpha} \tag{24}$$

Therefore, the horizontal force is simplified as

$$F_H = H_R + H_T \tag{25}$$

Table 13 - Parameters from tests 6 and 27, run at 0.1 and 2.7cm/s respectively

Parameter	**Test**		**Parameter**	**Test**	
	6 (0.1cm/s)	**27 (0.1cm/s)**		**6 (0.1cm/s)**	**27 (0.1cm/s)**
h	0.030m	0.030m	μ	0.5	
h_r	0.15m	0.13m	θ	37°	
g	9.81m/s^2		w	0.60m	
α	37°		ρ_i	900 kg/m^3	

With these parameters, the horizontal forces according to the proposed formulae should be $F_H = 89.9N$ for test 6 and $F_H = 81.0N$ for test 27, which are in the same range of the maximum load registered by the force transducers during these tests: $78N$ and $86N$ respectively. The force-time graph and a detail on the aspect of the ice over the breakwater on these tests can be observed in figures Figure 27 and Figure 28.

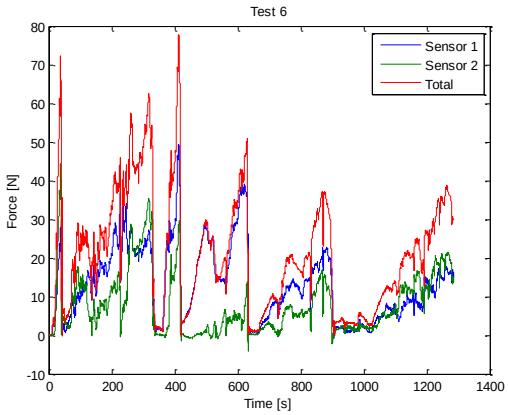

Figure 27 - Test 6. Force-time graph and detail on the ride up event

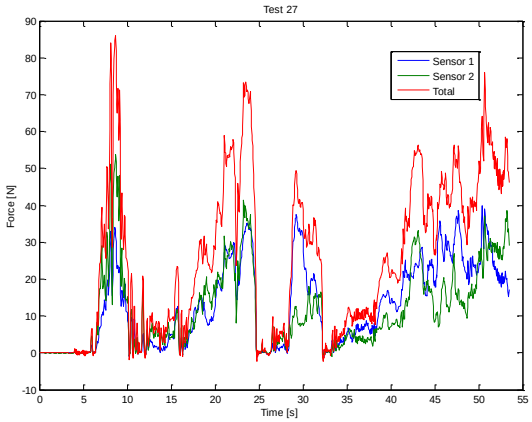

Figure 28 - Test 27. Force-time graph and detail on the ice accretion

This shows that the formulae proposed by ISO/FDIS 19906:2010(E) is a good approximation. However, the formulae do not consider the breaking length that, as shown in Table 12**¡Error! No se encuentra el origen de la referencia.**, strongly influences the horizontal load.

The ice-drift speed is not included in these formulae either. After observing Table 12, the drift speed does not have a consistent influence on the recorded loads, so we can say that these formulae are on the right track in this regard.

5 CONCLUSION AND RECOMMENDATION FOR FURTHER WORK

5.1 Conclusion

After the experimental work conducted to write this thesis and its comparison with earlier results, the following conclusions can be drawn concerning the prospective use of berm breakwaters in Arctic areas:

- Regarding the effects of the ice velocity when it approaches the breakwater. We can say that the speed does not seem to have a strong and constant influence in the magnitude of the ice loads on the breakwater. However, higher speeds increment the likeliness of local failures happening on the breakwater, as well as a change on the ice behaviour, like decreasing the probability of the ride up.

- A non-reshaped berm breakwater is not the ideal design for Arctic areas since small events causing local damage are expected to happen due to ice-sheets riding up the structure. These events have observed in more than fifty percent of the tests. A berm breakwater that allows reshaping is probably a more useful design.

- The irregular ice rubble formation (named realistic stacking by Mennessier (2012)) seems to be an effective barrier to the incoming ice. As seen in the tests, berm breakwaters usually provoke this behaviour, which is a helpful process to protect the breakwater and the structures behind it. This behaviour joins the earlier predicted pile up as a useful barrier against the incoming ice.

- Finally, the newly tested circular shaped ice floes with which the variation of the ice concentration was achieved, presented a completely different behaviour that the wide and rectangular ice floes that approached to the structure in a 2D scenario. The circular ice floes at concentrations around 8/10 were always accumulated in the slope of the breakwater, forming ice rubble that protected the structure and did not cause any apparent damage.

5.2 Recommendation for further work

After the experimental work conducted and the analysis of the results, some recommendation is given in order to delve deeper into the knowledge of the interaction between sea-ice and berm breakwaters.

- Concerning the experimental setup, some changes should be done in order to achieve global failures of the breakwater that gives us the ice load that it can really resist. A more powerful motor should be installed so higher speeds and loads can be tested. The force transducers should be able to record larger loads than the actual ones in order to record this loads and the stiffness of the pushing plate should also be higher.

- Regarding the new dimension added to the experiments with the ice concentration, the experimental setup can be improved. A way to push the ice that does not vary the concentration should be found on this regard. The small width of the flume was also a

strong limitation when trying to add a new dimension to the experiments due to the constraints of its walls.

- Last but not least, it would be interesting to run more tests to be able to analyse the likeliness of the events with statistical tools

REFERENCES

Chen, A.T. and Leidersdorf, C.B. (ed) (1988): *Arctic Coastal Processes and slope protection design.* Technical Council on Cold Regions Engineering Monograph. ASCE, 1988.

Daly, S.F., Zufelt, J., Zabiinski, L., Sodhi, D. and Bjella, K.(2008): *Estimation of ice impacts on armor stone revetments at Barrow, Alaska.* Proceedings of the 19th IAHR International Symposium on ice, Vancouver, British Columbia, Canada, July 6 – 11, 2008.

Gürtner, A. (2009): *Experimental and numerical investigations on ice-structure interaction*. PhD-thesis, Norwegian University of Science and Technology, Department of Civil and Transport Engineering, January 2009.

Hughes, S.A. (1993): *Physical models and laboratory techniques in coastal engineering*, World Scientific Publishing, Singapore.

ISO/FDIS 19906:2010(E). *Petroleum and natural gas industries – Arctic offshore structures*. Technical report, International Standard, International Standardization Organization, Geneva, Switzerland, 2010

Lengkeek, H.J., Croasdale, K.R. and Metge, M. (2003): *Design of ice protection barrier in Caspian Sea*. Proceedings 22nd International Conference on Offshore Mechanics and Arctic Engineering (OMAE03); June 8-13, 2003, Cancún, Mexico.

MacIntosh, K.J., Timco, G.W. and Willis, D.H. (1995): *Canadian experience with ice and armour stone*. Proceedings of the 1995 Canadian Coastal Conference, Dartmouth; Nova Scotia, October 1995. Vol. 2, pp 597-606.

Martin Vide, J.P (2006): *Ingeniería de Ríos*. 2nd edition. Edicions de la Universitat Politècnica de Catalunya; Barcelona, December 2006. Pp 330-335.

Mennessier, T. (2011): *Berm breakwaters as protection of harbours, artificial islands and shorelines in Arctic areas, Project work*, Norwegian University of Science and Technology, Department of Civil and Transport Engineering, December 2011.

Mennessier, T. (2012): *Berm Breakwaters as Protection of Harbours, Artificial Islands and Shorelines in Arctic Areas, Master Thesis*, Norwegian University of Science and Technology, Department of Civil and Transport Engineering, June 2012.

Sackinger, Wm. (1985): *Ice action against rock mound structure slopes*. In Per Bruun (ed): Design and construction of mounds for breakwaters and coastal protection. Elsevier.

Sodhi, D.S., Borland, S.L. and Stanley, J.M. (1996): *Ice action on riprap. Small-scale tests*. US Army Corps of Engineers, Cold Regions Research&Engineering Laboratory. CRREL Report 96-12.

Tørum, A. (2009). *Coastal Structures, Lecture notes for TBA 4145 Port and Coastal Facilities*, Norwegian University of Science and Technology, Department of Civil and Transport Engineering, 2009.

Timco, G. W., Willis, D.H. and Wright, B.D. (1995): *Ice action on armor rocks with application to an artificial island concept*. Proceedings of the Second International Conference on Development of Russian Arctic Offshore, RAO'95, St. Petersburg, Russia, 1995.

LIST OF SYMBOLS

Roman letters

D	diameter of the ice floe
$D_{n50} = \sqrt[3]{\frac{W_{50}}{\rho_s}}$	nominal diameter of the median stone
E	Young's modulus
Fr	Froude Number
F_H	horizontal component of ice action
F_V	vertical component of ice action
H_B	breaking load of the ice sheet
H_L	load required to lift the ice rubble on top of the advancing ice sheet prior to breaking it
H_P	load component required to push the sheet ice through the ice rubble
H_R	load to push the ice blocks up the slope through the ice rubble
H_T	load to turn the ice block at the top of the slope
c	cohesion angle of the ice rubble.
e	porosity of the ice rubble
g	acceleration of gravity
h	thickness of the ice sheet
h_b	water depth on berm (negative means berm is above S.W.L)
h_r	rubble height
l	length of the flume covered by ice
L	length
Re	Reynolds Number

R^2	Pearson product moment correlation coefficient
U	particle's velocity
$\bar{x}$	arithmetic mean
w	width of the breakwater
W	width of the flume covered by ice

Greek letters

α	slope angle of the breakwater
λ	geometrical scale ratio
μ_i	ice-to-ice friction coefficient
θ	angle the rubble makes with the horizontal
ν	Poisson ratio
ρ_i	density of the ice
ρ_s	density of stone
ρ_w	density of water
σ	standard deviation
σ_f	flexural strength of the ice sheet
ϕ	friction angle of the ice rubble

APPENDIX: RECORDED FORCE FOR ALL THE TESTS

A time-force graphic has been generated for every test carried out during the experimental work. All of them are compiled in this appendix.

Each graph shows the time in the horizontal axis. The force registered by each transducer, as well as the total force are shown in the vertical axis. The recording of negative force values corresponds to the moment originated by the accumulation of ice under the water surface in front of the pushing plate.

The graphs corresponding to the tests carried out with the rectangular ice floes are displayed in a way that it is easy to visually compare the results of the tests carried out at high/low ice drift speed for ice flows with identical characteristics.

All the tests carried out with the circular shaped ice floes were conducted at the same drift speed, 2.7cm/s. Because of that, they are displayed in a way that it is possible to compare the graphs of the tests carried out with the same ice flows but with different roughness.

To facilitate the identification of the characteristics of every test Table 4 - Groups of tests. **¡Error! No se encuentra el origen de la referencia.**is shown again.

Table 14 - Groups of tests (bis)

Shape		**Rectangular**			
Thickness (cm)		**1,5**		**3**	
Roughness (µm)		**150**		**150**	
Drift speed (cm/s)		**0,1**	**2,7**	**0,1**	**2,7**
Length (cm)	**7,5**	TestR1LABC.F1	TestsR1HABC.F11,12,13	TestR2LA.F5	TestsR2HA.F23,24,25
	10,5			TestR2LB.F6	TestsR2HB.F26,27,28
	13,5			TestR2LC.F7	TestsR2HC.F29,30,31
	16,5	TestR1LD.F2	TestsR1HD.F14,15,16	TestR2LD.F8	TestsR2HD.F32,33,34
	19,5	TestR1LE.F3	TestsR1HE.F17,18,19	TestR2LE.F9	TestsR2HE.F35,36,37
	22,5	TestR1LF.F4	TestsR1HF.F20,21,22	TestR2LF.F10	TestsR2HF.F38,39,40

Shape		**Circular**			
Thickness (cm)		**1,5**		**3**	
Roughness (µm)		**0**	**150**	**0**	**150**
Drift speed (cm/s)		**2,7**			
Diameter (cm)	13,5	TestsC1HC.N41,42,43	TestC1HC.F60	TestsC2HC.N44,45	TestsC2HC.F55
	22	TestsC1HF.N46,47	TestC1HF.F61	TestC2HF.N48	TestC2HF.F56
	13,5 and 22	TestsC1HCF.N	TestsC1HCF.F	TestsC2HCF.N	TestsC2HCF.F

		49,50,51	62,63,64	52,53,54	57,58,59

TEST R1LABC.F

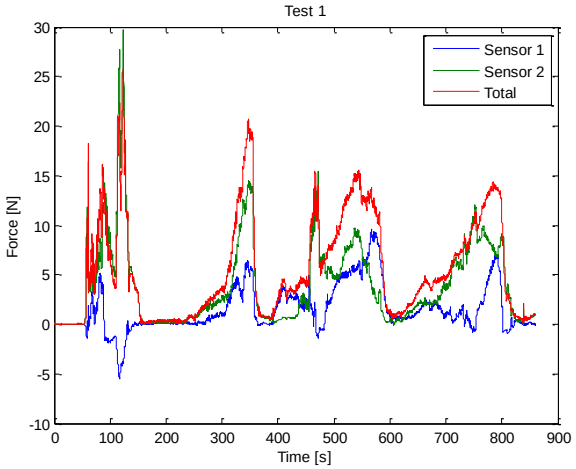

TESTS R1HABC.F

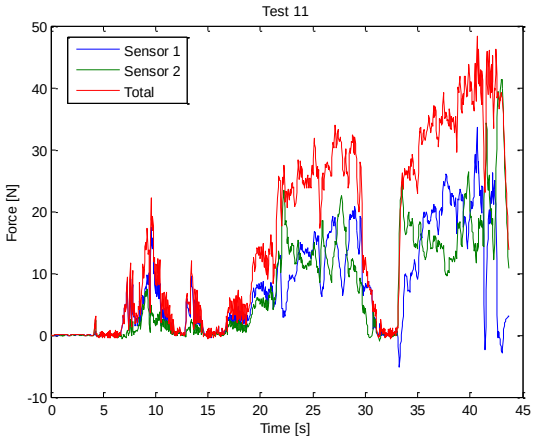

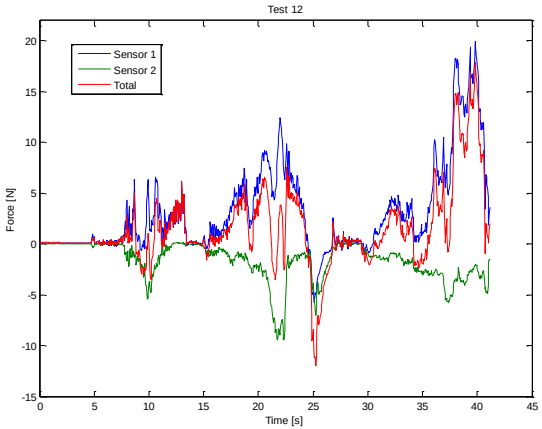

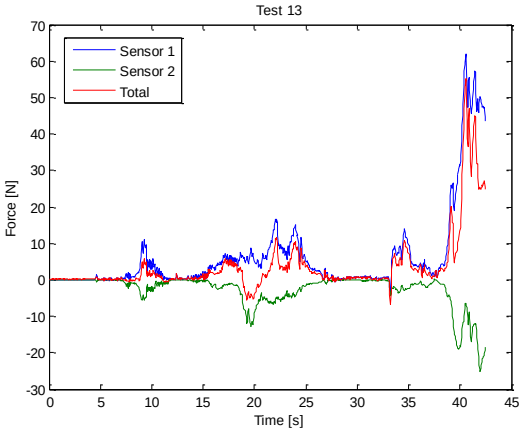

TEST R1LD.F

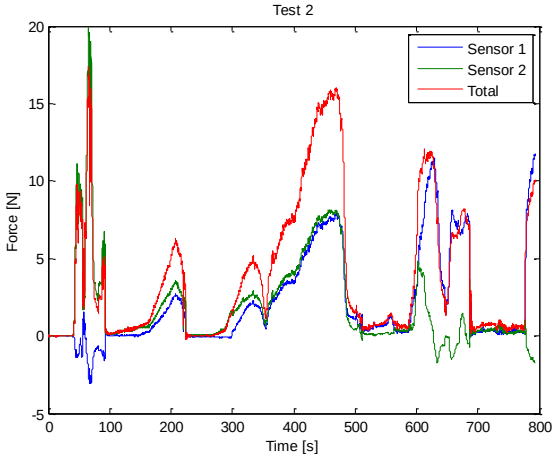

TESTS R1HD.F

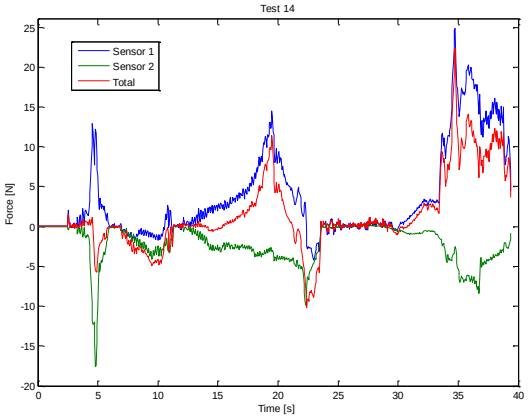

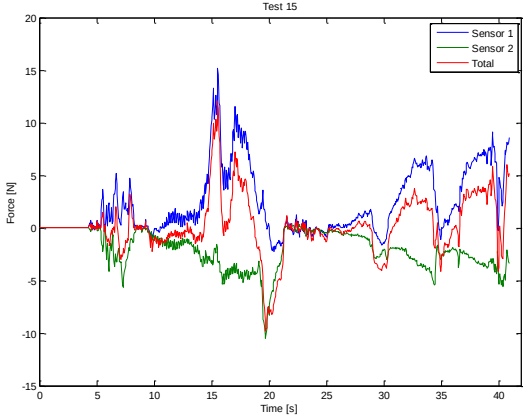

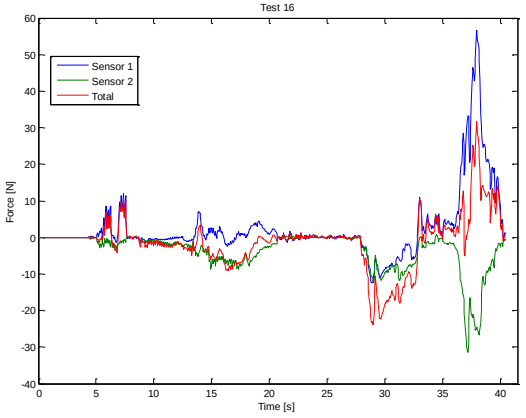

TEST R1LE.F

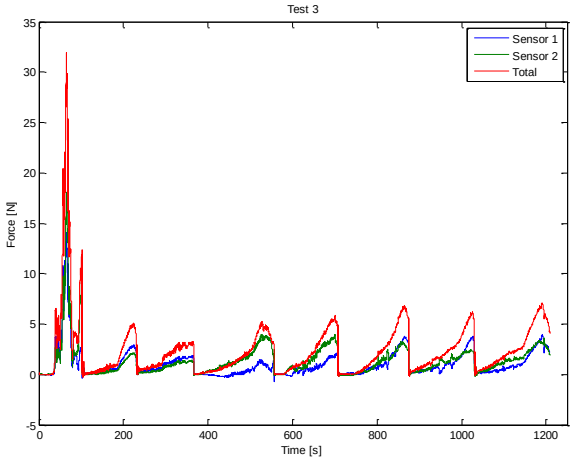

TESTS R1HE.F

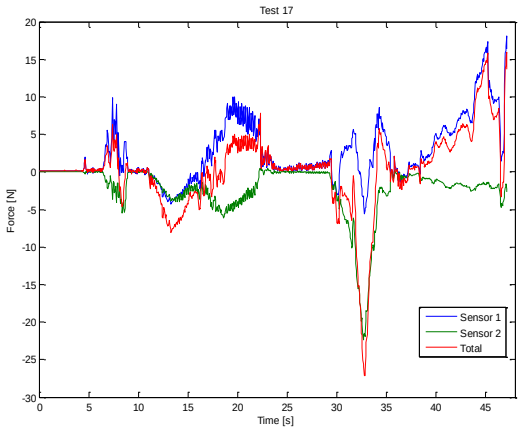

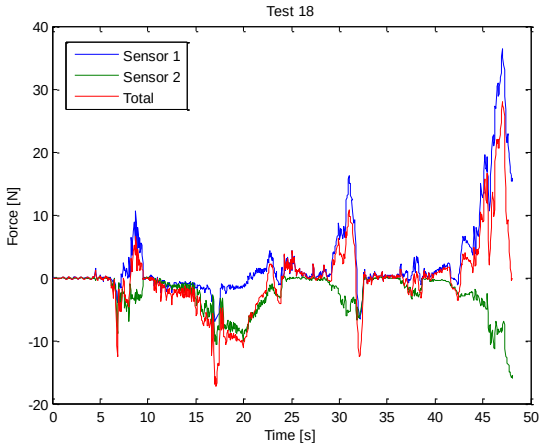

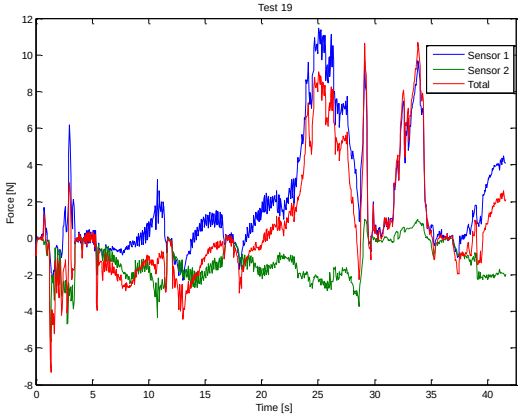

TEST R1LF.F

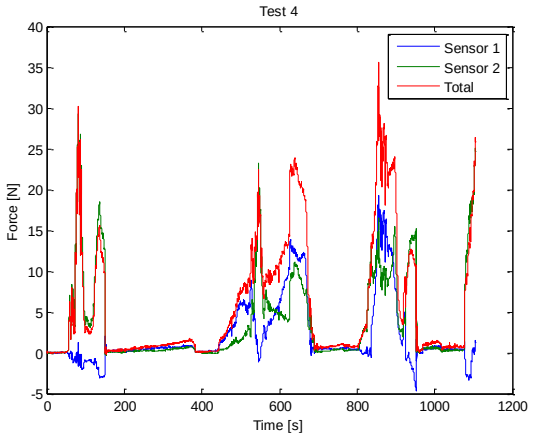

TESTS R1HF.F

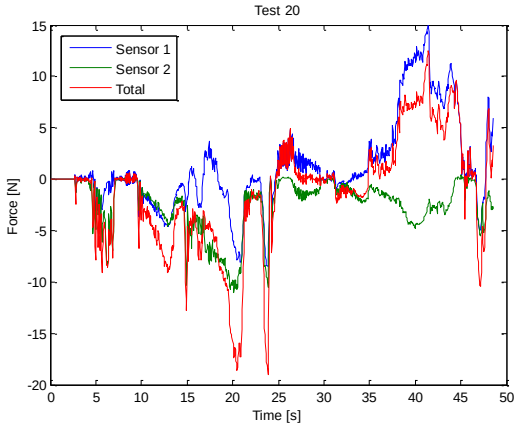

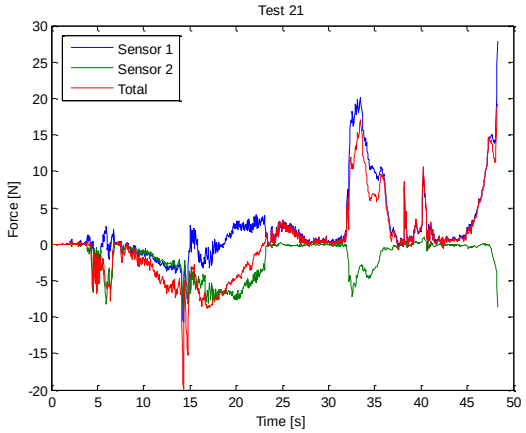

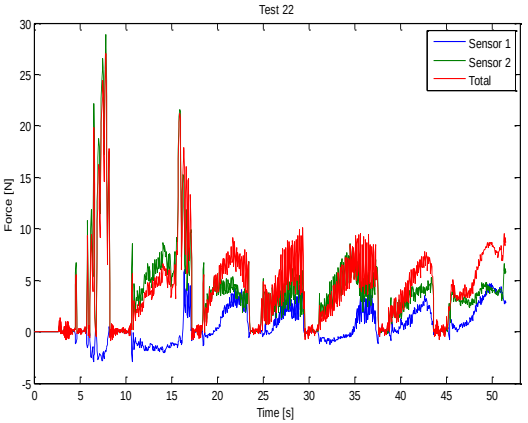

TEST R2LA.F

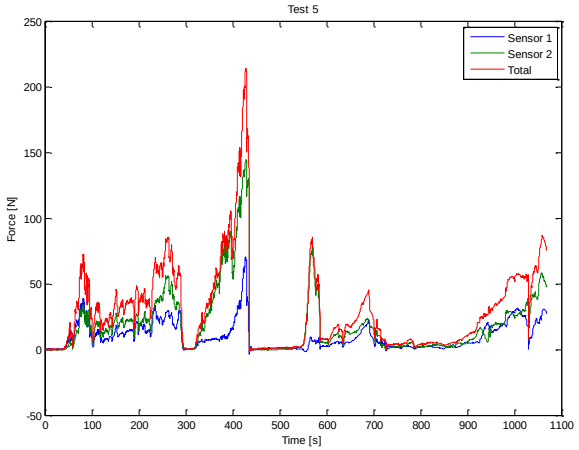

TESTS R2HA.F

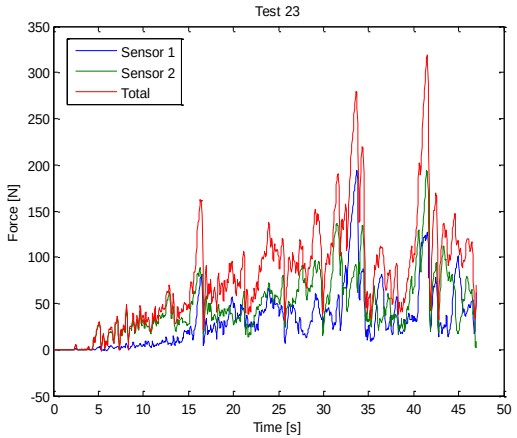

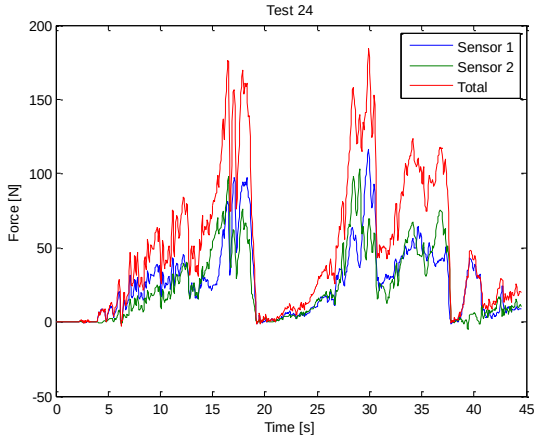

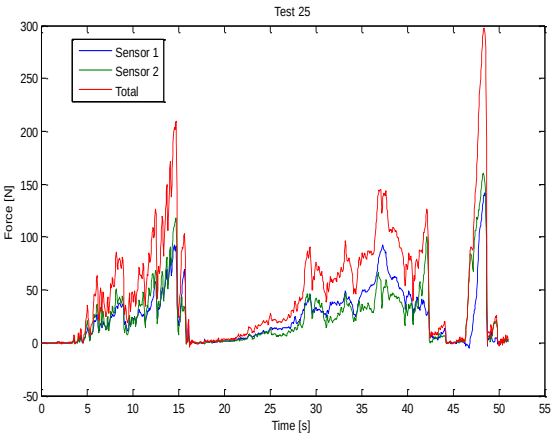

TEST R2LBF

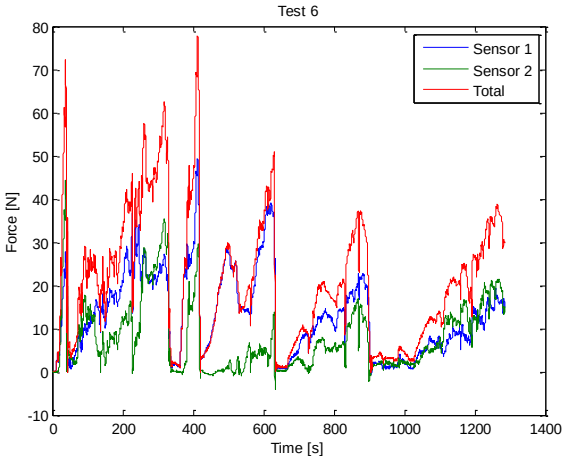

TESTS R2HB.F

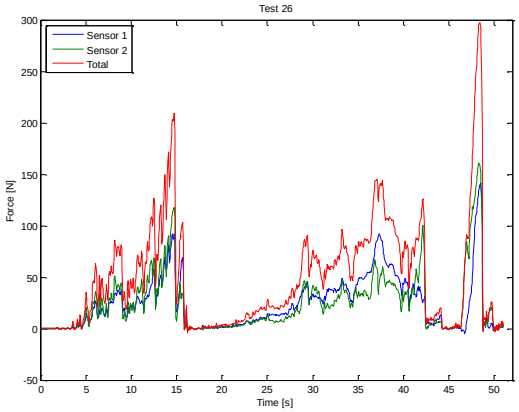

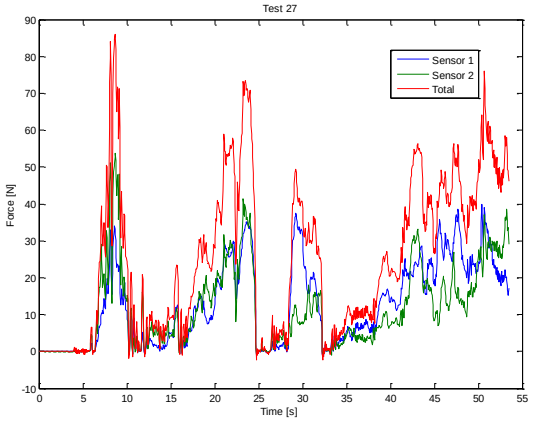

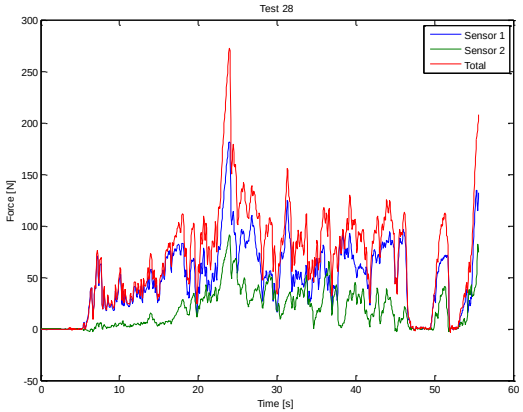

TEST R2LC.F

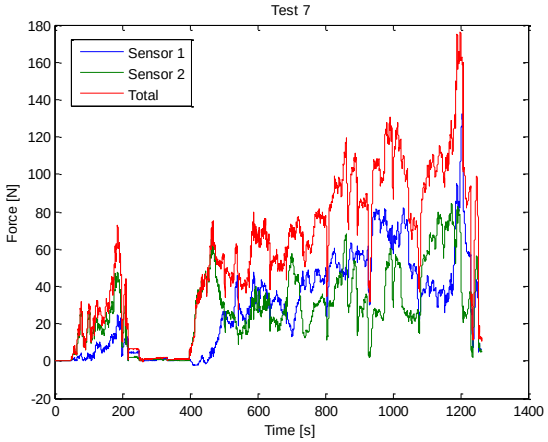

TESTS R2HC.F

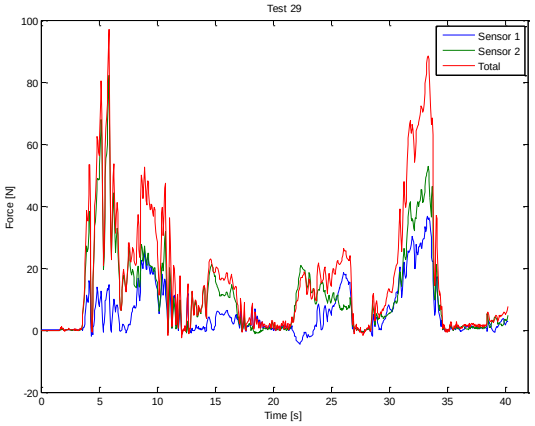

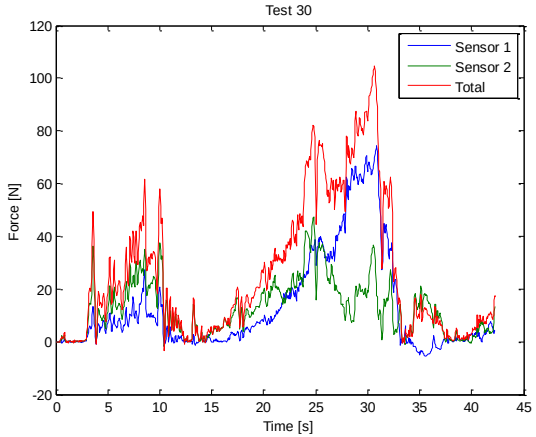

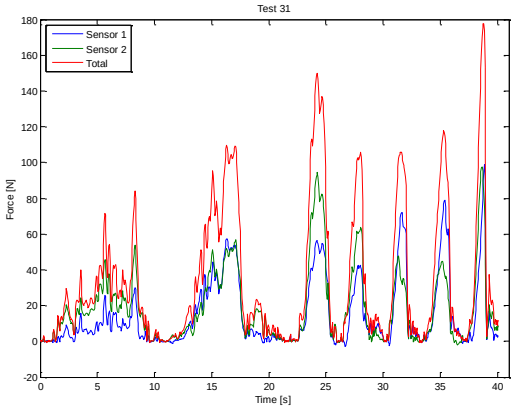

TEST R2LD.F

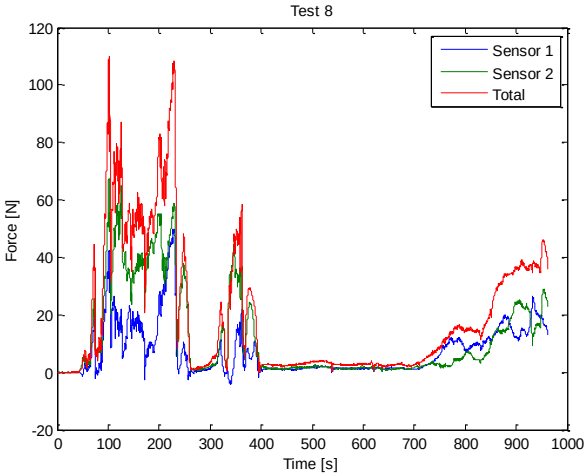

TESTS R2HD.F

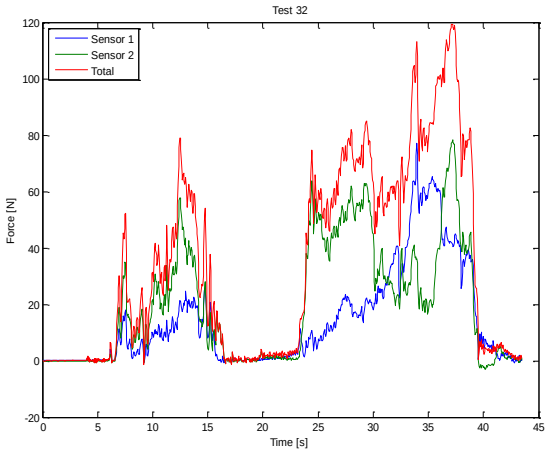

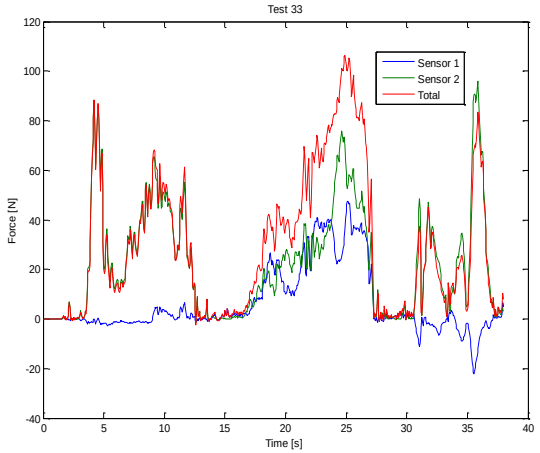

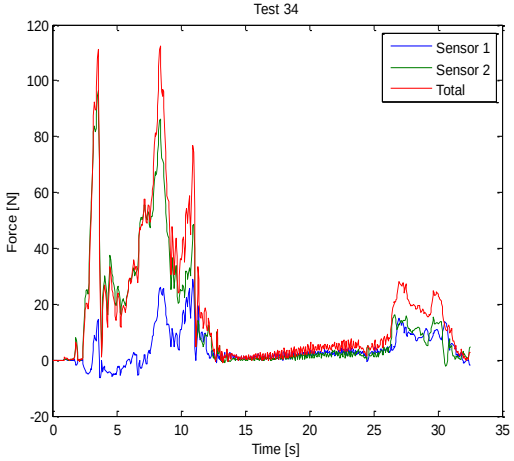

TEST R2LE.F

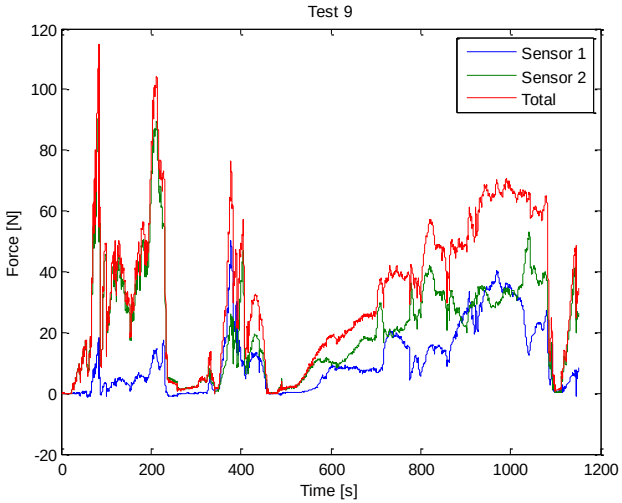

TESTS R2HE.F

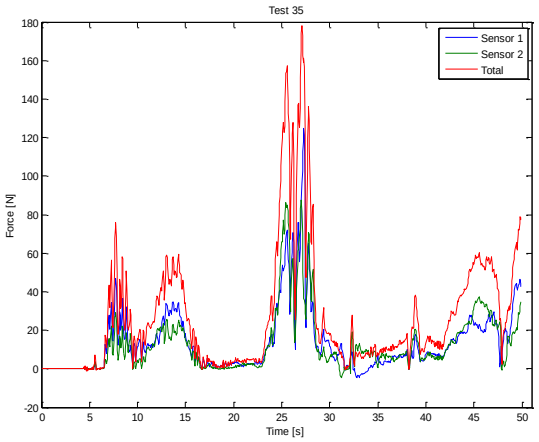

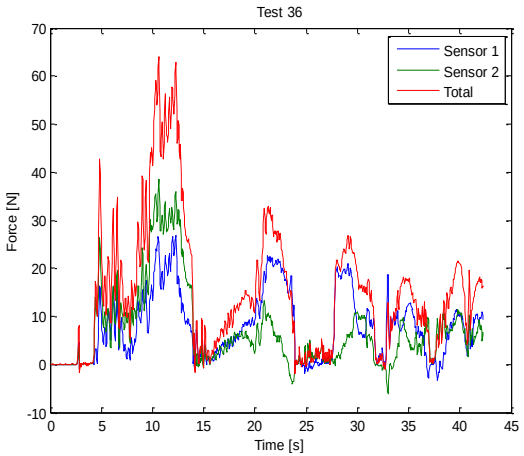

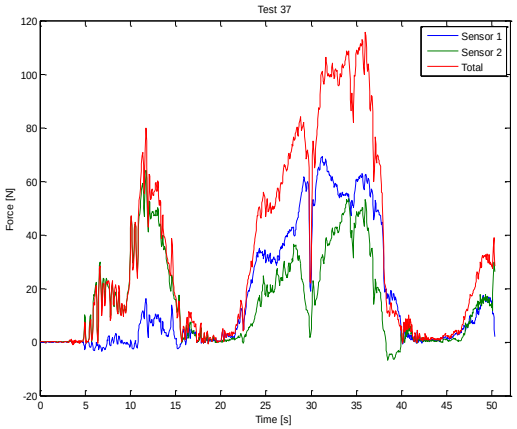

TEST R2LF.F

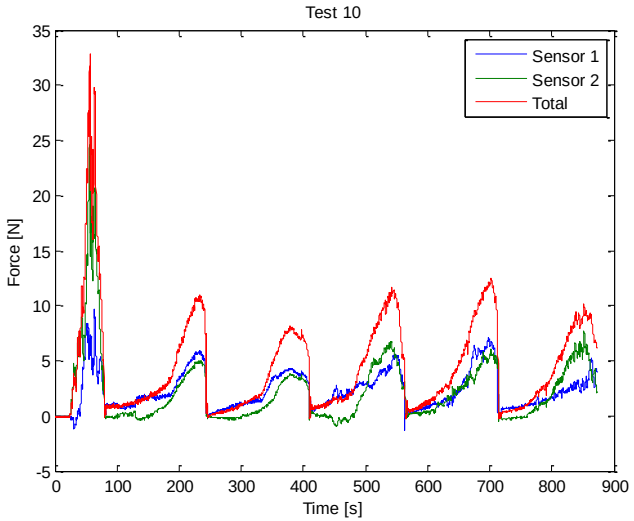

TESTS R2HF.F

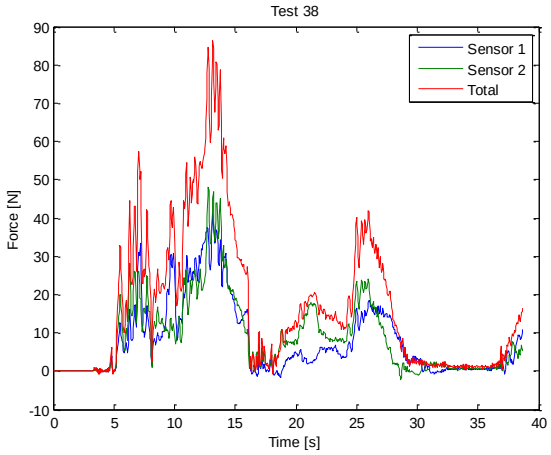

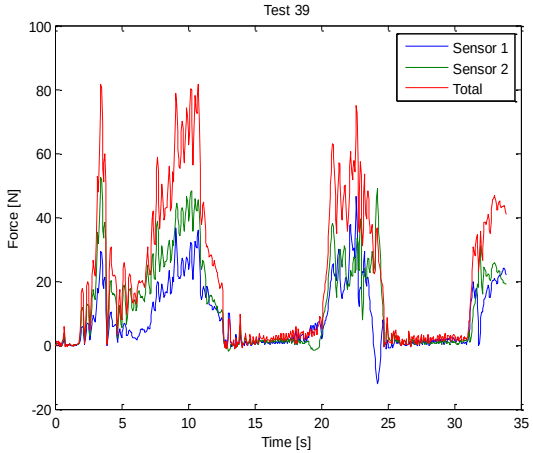

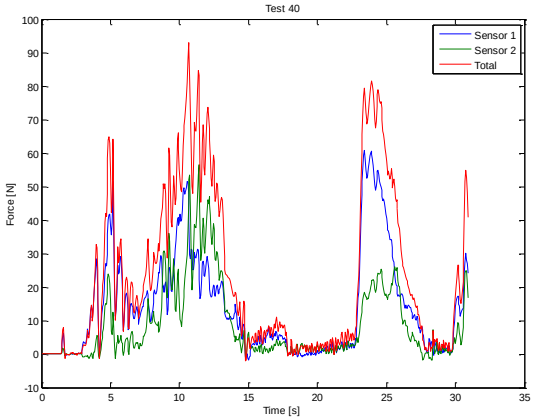

TESTS C1HC.N

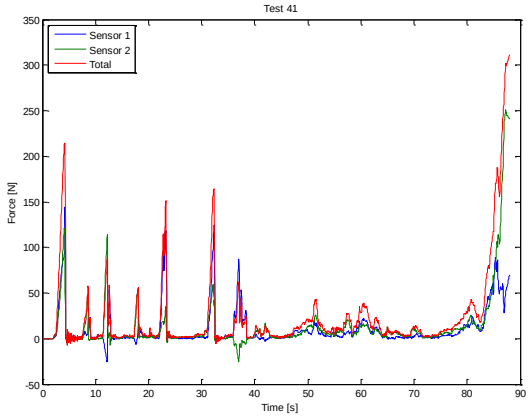

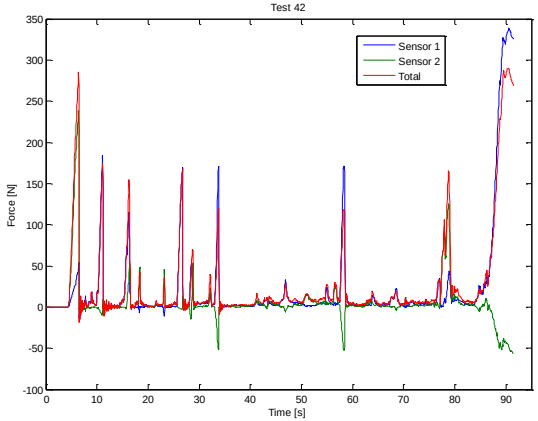

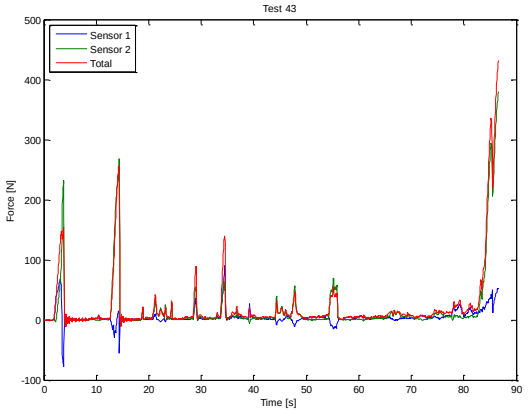

TESTS C1HC.F

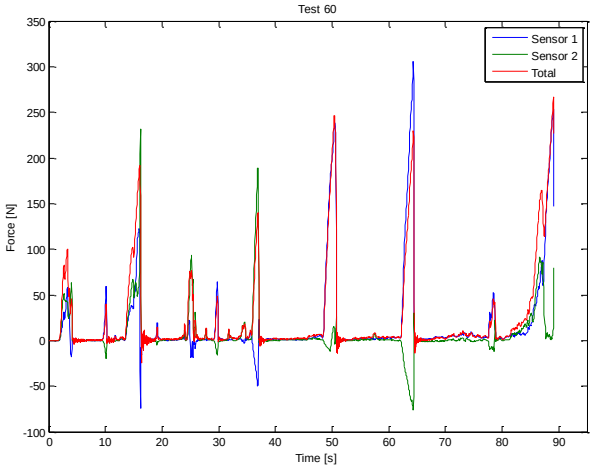

TESTS C1HF.N

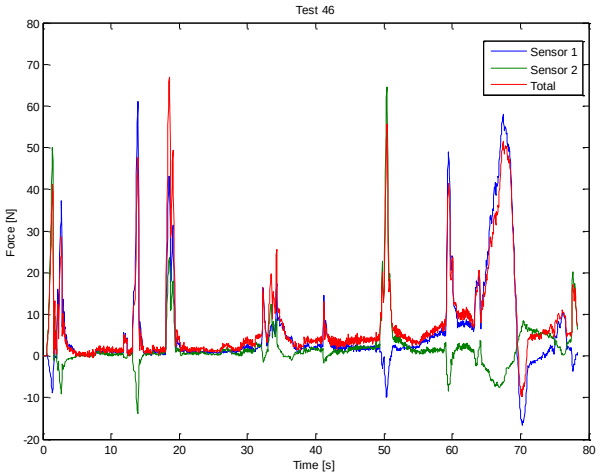

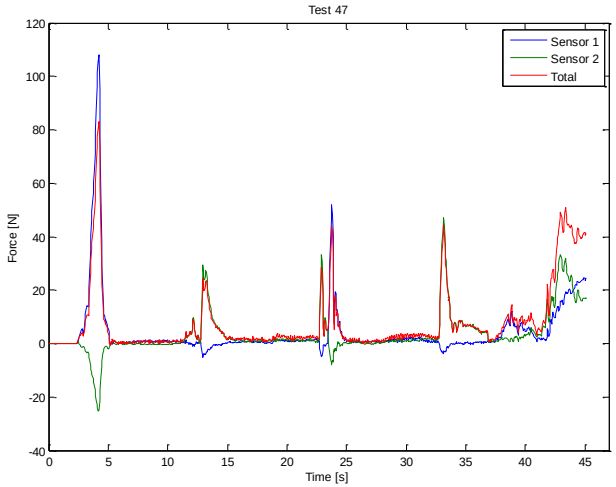

TESTS C1HF.F

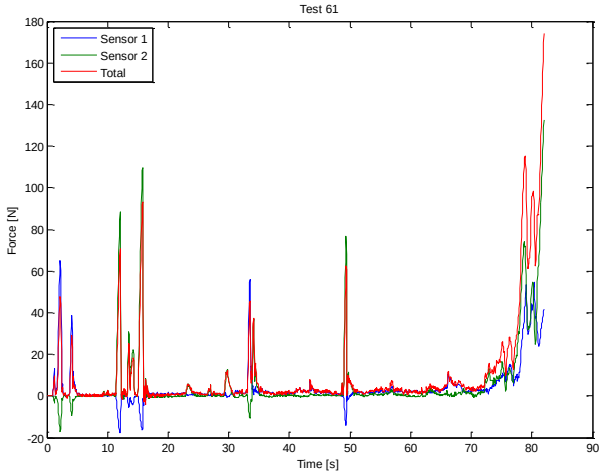

TESTS C2HC.N

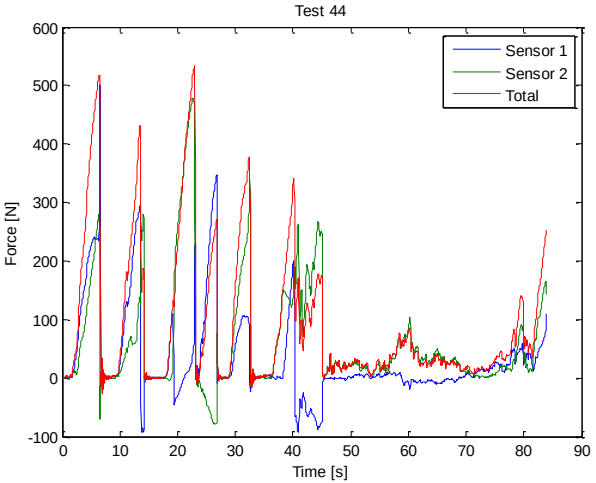

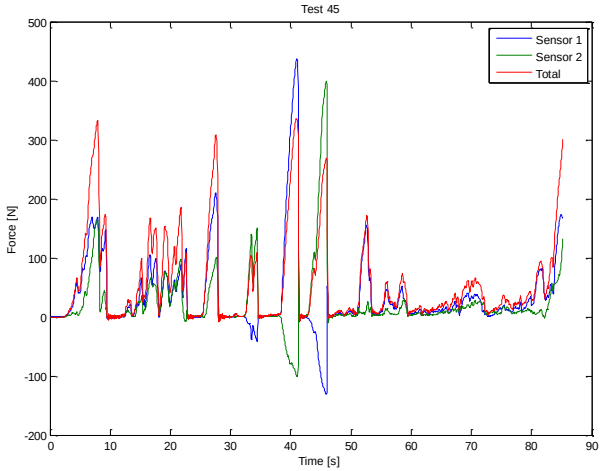

TEST C2HC.F

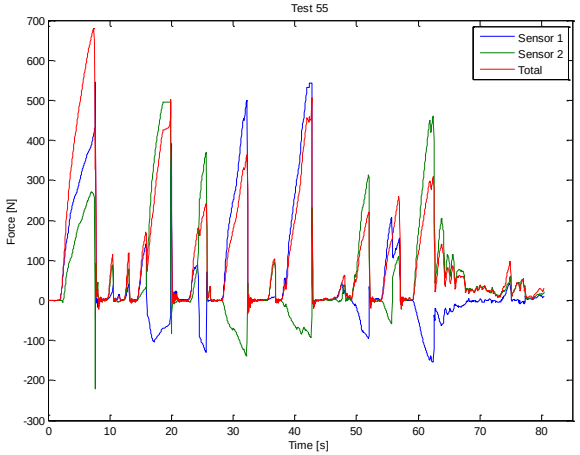

TEST C2HF.N

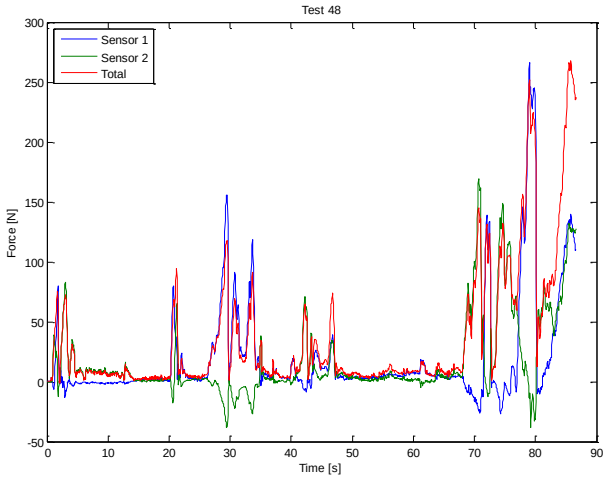

TEST C2HF.F

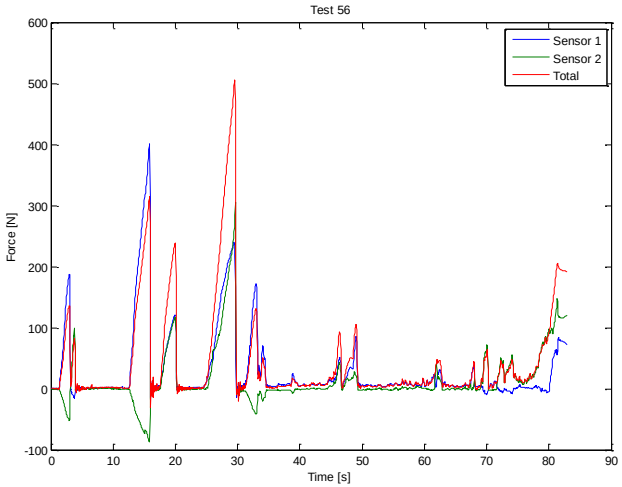

TESTS C1HCF.N

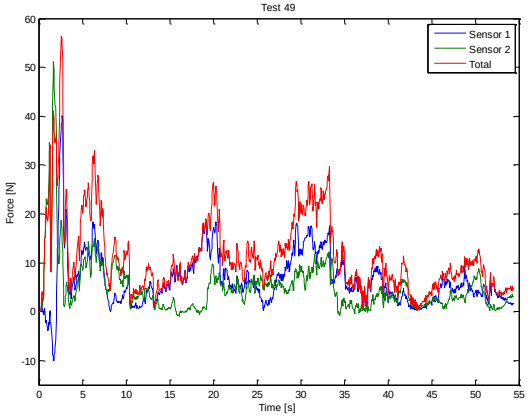

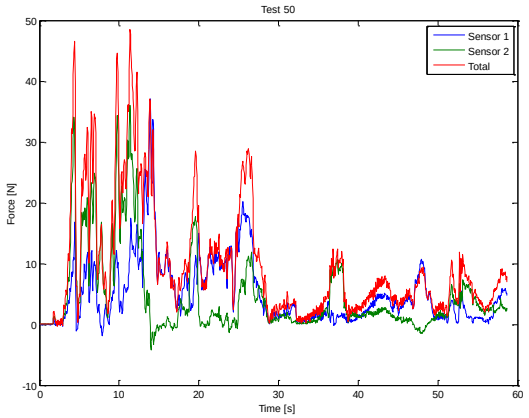

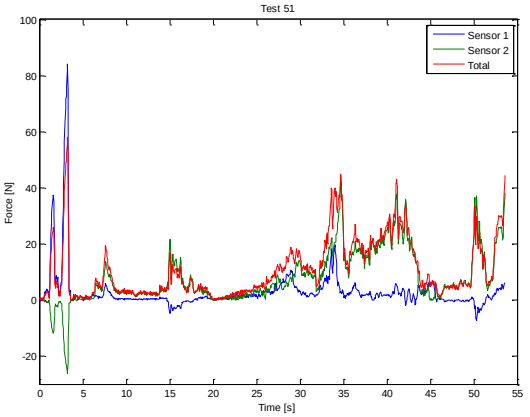

TESTS C1HCF.F

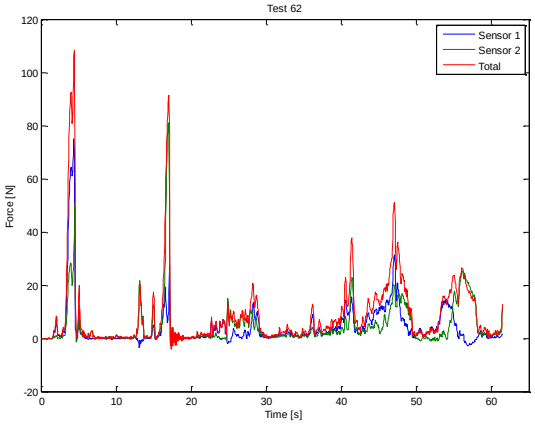

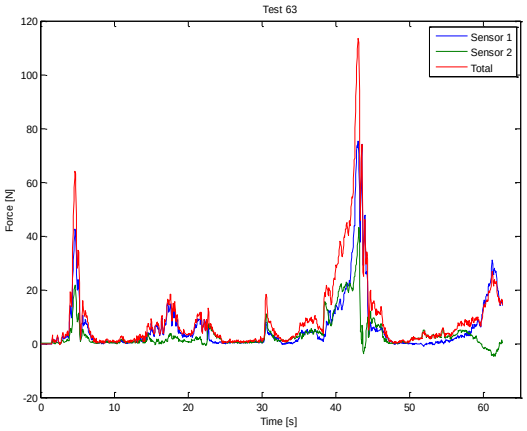

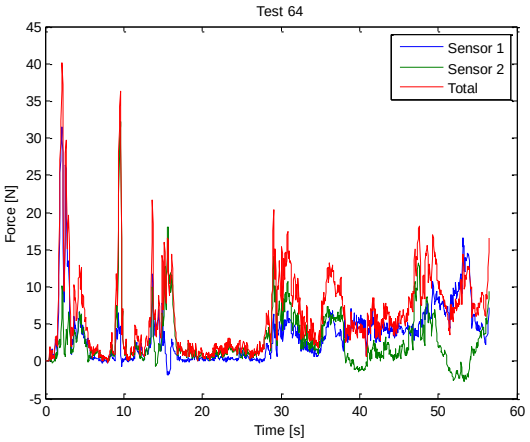

TESTS C2HCF.N

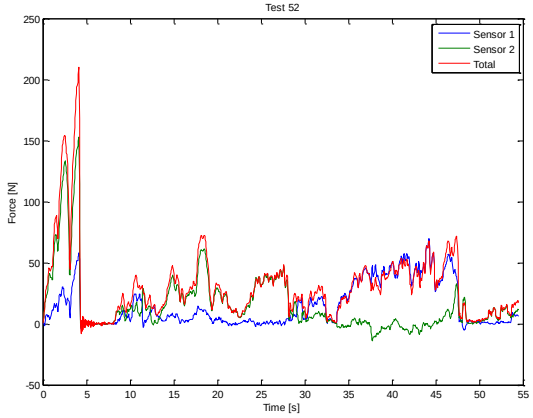

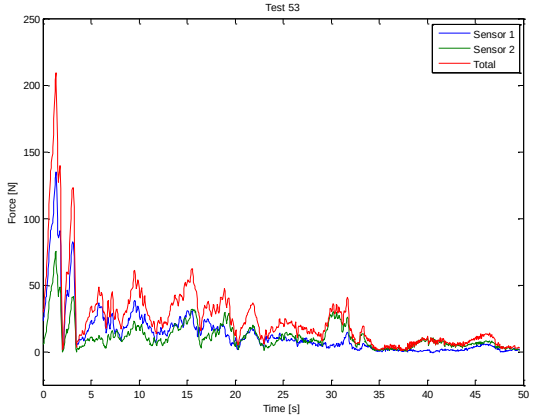

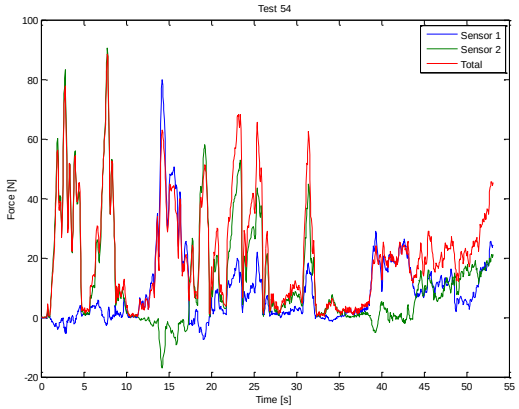

TESTS C2HCF.F